Journal of Molecular Spectroscopy 328 (2016) 7–26

Contents lists available at ScienceDirect

Journal of Molecular Spectroscopy

journal homepage: www.elsevier.com/locate/jms

Spectroscopy underlying microwave remote sensing of atmospheric water vapor

M.Yu. Tretyakov

Institute of Applied Physics of RAS, 46 Ul'yanov Street, 603950 Nizhniy Novgorod, Russia

ARTICLE INFO

Article history:
Received 27 April 2016
In revised form 15 June 2016
Accepted 18 June 2016
Available online 21 June 2016

Keywords:
Atmosphere
Water vapor
Diagnostic lines
Radiation absorption
Continuum
Radiometry
Molecular spectroscopy

ABSTRACT

The paper presents a spectroscopist's view on the problem of recovery of the atmosphere humidity profile using modern microwave radiometers. Fundamental equations, including the description of their limitations, related to modeling of atmospheric water vapor absorption are given. A review of all reported to date experimental studies aimed at obtaining corresponding numerical parameters is presented. Best estimates of these parameters related to the Voigt (Lorentz, Gross, Van Vleck – Weisskopf and other equivalent) profile based modeling of the 22- and 183-GHz water vapor diagnostic lines and to non-resonance absorption as well as corresponding uncertainties are made on the basis of their comparative analysis.

0. Introduction

Water is one of the key molecules that determine the physical and chemical processes in Earth's atmosphere. Constituting less than 0.5% of the atmosphere's mass, water is responsible for about 70% of the radiation absorbed by the atmosphere, thus having a major impact on the radiation balance (see, for example [1,2]). Moreover, water vapor is a primary greenhouse gas in the Earth's atmosphere that produces a positive feedback, determining the weather and affecting global climate change [3].

Water molecules comprising the atmospheric water vapor absorb radiation in the whole wavelength range from radio to ultraviolet and beyond. This absorption is mainly due to the transition of molecules to higher vibrational and rotational energy levels corresponding to resonance spectral lines. These lines are rather intense, as the water molecule, being of low molecular weight, has a large permanent dipole moment. Since H_2O is a light and very non-rigid asymmetric top molecule, its resonance lines are quite evenly distributed over the entire spectrum of electromagnetic waves. There are two mechanisms allowing the atmospheric water vapor to accumulate a considerable amount of energy and carry it with the air flow over long distances on a planetary scale. These are (a) the condensation of molecules with a possible subsequent transition into the solid phase, starting with the collisional formation of double molecules, and (b) the energy distribution over internal degrees of freedom of the molecules. It is impossible to distinguish which of these two mechanisms plays the primary role. Qualitative estimations show that the distribution of roles between them may strongly depend on the weather conditions of a particular region. Due to its geometric structure, the water molecule has a relatively large (for the most common atmospheric molecules) number of the vibrational and rotational degrees of freedom - three vibrational and three rotational degrees of freedom. Internal energy accumulated by the atmospheric water vapor presumably has an influence on the formation and dynamics of tropical cyclones and is of importance not only for predicting rainfall amount, but also for early warning of possible extreme weather events. Precise, continuous quantitative information on the spatial distribution of atmospheric humidity is of prime priority for weather forecasting and monitoring of global climate change [4]. The most complete information of this kind on a global scale can be obtained from satellite remote sensing. The currently available network of specialized satellites provides global maps of the integrated thermal emission of the atmosphere at frequencies near the spectral lines corresponding to the lowest-frequency rotational transitions of water molecules (see, e.g. [5–7], and references therein). The characteristics of this radiation are unequivocally associated with the vertical profile of the absorption coefficient of water vapor, which is dependent on the concentration of water molecules, frequency, temperature, pressure, etc. However, a model of radiation propagation in the atmosphere is required to

E-mail address: trt@ipfran.ru
URL: http://www.mwl.sci-nnov.ru/

http://dx.doi.org/10.1016/j.jms.2016.06.006
0022-2852/

retrieve the quantitative information from satellite data. The rigor and accuracy of the model determines the accuracy of water vapor concentration retrieval. Any theoretical model requires knowledge of numerical coefficients, which are the model's parameters. Their values are usually found in experiment. It is obvious that most of the parameters are model-dependent. Improving the accuracy of their determination will increase the accuracy of modeling only in proportion to the "weight" of this parameter in the model, and only as long as the model can be considered adequate to the object or process being modeled. To be able to critically evaluate the modeling results, it is important to thoroughly understand the underlying principles of the model, its physical limitations, and the meaning of its numerical coefficients. Key aspects of molecular gas spectroscopy used for modeling of the atmospheric absorption are discussed in the first section of this paper. The second section analyzes the experimental data accumulated to date by the international research community, which provide the selected models with a set of numerical parameters required for quantitative modeling of the absorption. The third section presents a comparative analysis of these data. Finally, on the basis of this analysis, conclusions are made about the most promising frequency bands for satellite remote sensing of atmospheric water vapor.

1. Fundamentals of atmospheric absorption modeling

The fundamental law of variation of the power of radiation as it passes through a medium (in a particular case, through the atmosphere or its separate gas constituent) was formulated by Pierre Bouguer (1698–1758)

$$W(l) = W_0 \cdot \exp(-\alpha \cdot l), \tag{1}$$

where W is the transmitted radiation power passed through a matter, W_0 is the incident power, l is the radiation path length, and α is the absorption coefficient which is dependent on the radiation frequency and is actually the absorption spectrum of the matter. Note that it follows from classical Maxwell equations that the absorption coefficient is directly proportional to the imaginary part of the refractive index of the medium. The absorption coefficient and the real part of the refractive index are related to each other through the Kramers – Kronig relations. Depending on measurement method the retrieved value of the gas absorption coefficient can or cannot be affected by the refractive index. In the former case proper corrections should be carefully determined and taken into account.

The gas absorption spectrum is the sum of the resonant and non-resonant absorption. The resonant absorption is a property of individual, non-interacting molecules. It corresponds to the ideal gas, in which the collision of molecules with each other occurs instantly and fully elastically, and the gas is permanently in the state of thermodynamic equilibrium. The resonant absorption occurs at certain frequencies associated with the change in the angular velocity of the molecule (rotational transition) or the oscillation frequency (vibrational transition). The non-resonant absorption arises from the interaction of molecules with each other, i.e. due to the non-ideality of gas. Even during a collision that can be regarded as almost elastic from the classical point of view, the field of one molecule causes a redistribution of charges in the other, resulting in a small transient induced dipole moment. Non-elastic collisions lead to a short-term "adhesion" of molecules, and the formation of a new radiation-absorbing object. In both cases, a new additional absorption mechanism takes place, which acts for a very short time and, consequently, is characterized in the spectral region by smooth, compared to the resonance lines, frequency dependences, therefore leading to the non-resonance absorption. Thus, the gas absorption coefficient can be expressed as the sum of the resonance lines and the non-resonance absorption resulting from non-elastic interactions of molecules

$$\alpha_{total} = \sum \alpha_{line} + \alpha_{non\text{-}resonance}. \tag{2}$$

1.1. Modeling of resonance lines of atmospheric water vapor

Water molecules in the Earth's atmosphere are almost entirely concentrated in the layer closest to the Earth's surface of about 10–15 km. Under these conditions, the shape of the resonance lines is completely determined by binary collisions, and the Doppler broadening can be neglected. The most popular shapes of the collision-broadened resonance line used to model absorption by atmospheric gases were comparatively analyzed in [8]. For this purpose, high-quality experimental data [9] on water vapor absorption near 22 GHz in air at atmospheric pressure were used. The analysis convincingly showed that the experimentally observed line best of all can be modeled by the van Vleck–Weisskopf profile [10]

$$\alpha_{line}(\nu, \nu_c) = \frac{S}{\pi}\left(\frac{\nu}{\nu_c}\right)^2\left(\frac{\Delta\nu}{(\nu-\nu_c)^2+\Delta\nu^2}+\frac{\Delta\nu}{(\nu+\nu_c)^2+\Delta\nu^2}\right), \tag{3}$$

where ν is the frequency of radiation, and ν_c, $\Delta\nu$ and S are parameters of the line profile, which are the frequency of the center, the half-width at half amplitude and the integrated line intensity, respectively. A better, compared to other models, fit of the profile (3) to the observed resonance line shapes in wide-range experimental spectrum recordings of humid air at atmospheric or near-atmospheric pressures was also reported in [11,12].

The profile (3) was actually derived for ideal gas molecules, assuming that only two molecules are involved in each collision, and the collisions are considered instant and elastic. It was shown in [13] that the finite duration of the collision of molecules τ_c in real gas means that the profile (3) is valid only when the frequency detuning satisfies $|\nu - \nu_c| \ll (2\pi\tau_c)^{-1}$. The smooth abruption of interaction of molecules with radiation during the collision leads to much faster decay of the line wing at detunings $|\nu - \nu_c| > (2\pi\tau_c)^{-1}$ in comparison with function (3) (so called sub-Lorentzian behavior). However, real shape of line wings at large detunings is not known yet in spite of considerable theoretical efforts. The simplest way of modeling the resonance line absorption in this situation is just cutting the wings at $(2\pi\tau_c)^{-1}$ assuming zero absorption at larger detunings (line wings cut-off). This procedure leads to unavoidable uncertainty in the non-resonance absorption determination, which will be discussed in Section 1.2. For the cut-off frequency it has been proposed [14] to use a value of 25 cm^{-1} (750 GHz). This corresponds to the time ($\sim 2 \cdot 10^{-13}$ s) needed for a water molecule moving at an average relative thermal speed at room temperature to fly a distance of 1.77 Å, which exceeds the maximum geometric size of the water molecule (~1.2 Å), but is less than the radius of the excluded gas-kinetic volume (~2.5 Å) and several times less than the spectroscopically determined radius of the collisional interaction cross-section between molecules. The choice of the maximum detuning is rather arbitrary, because its verification is currently impossible either by experimental methods or by first-principles calculations. The above evaluations show that the value of 25 cm^{-1} is rather close to the upper limit, but nonetheless is used in such well known propagation models as MPM [15] and MonoRTM [16].

All resonance line parameters defining the profile (3) are functions of temperature and pressure. The integrated intensity is directly proportional to the concentration of absorbing molecules, i.e. in the considered case – to the partial pressure of water vapor in the atmosphere. Its temperature dependence is given by the

change in the statistical weight of the lower state of the transition and by Boltzmann factors determining the population of molecular energy levels corresponding to the transition which are calculated from the energy of the lower level and the frequency of the corresponding transition (see, e.g. [17]):

$$S(T) = S(T_0)\left(\frac{T_0}{T}\right)^{2.5} \exp\left(\frac{E_{low}}{kT_0}\left(1-\frac{T_0}{T}\right)\right), \quad (4)$$

where k is the Boltzmann's constant, E_{low} is the energy of the lower level, and $S(T_0)$ is the integrated intensity at a given temperature.

For the linewidth and the line center frequency, the following relations within binary collision approximation are valid:

$$\begin{aligned} \Delta\nu &= \gamma_w p_w + \gamma_{air} p_{air}, \\ \nu_c - \nu_0 &= \delta_w p_w + \delta_{air} p_{air}, \end{aligned} \quad (5)$$

where p_w and p_{air} are partial pressures of water vapor and air, γ_w, γ_{air} and δ_{air}, δ_w are parameters of broadening and shifting of the water line of interest by water vapor pressure and dry air pressure, respectively, and ν_0 is the "zero pressure" transition frequency.

Power functions are commonly used to account for the temperature dependence of the collision parameters. For the broadening and shifting, for example, they look as follows:

$$\gamma(T) = \gamma(T_0)\cdot\left(\frac{T_0}{T}\right)^{n_\gamma}, \quad \delta(T) = \delta(T_0)\cdot\left(\frac{T_0}{T}\right)^{n_\delta}, \quad (6)$$

where $\gamma(T_0)$ and $\delta(T_0)$ are values of corresponding parameters at a given temperature T_0. These functions are the simplest approximations of actual dependencies near T_0, that work quite well with detunings from T_0 by 30–50 K, which is sufficient for atmospheric applications. Most experimental data on the line parameters are obtained within some temperature range near room temperature. This explains why the values of 296 K or 300 K are chosen for T_0 in the propagation models.

Parameters that most significantly affect the atmospheric molecular line shape, including ν_0, $\gamma_w(T_0)$, $\gamma_{air}(T_0)$, $\delta_{air}(T_0)$, $n_\gamma{}^{\text{air}}$, E_{low} and $S(T_0)$ (which is given as normalized to the concentration of absorbing molecules) can be found in many databases specialized for spectroscopic applications, among which the most popular is HITRAN [18] (http://HITRAN.org).

It should be noted that high-accuracy resonance absorption modeling is needed to solve some problems of satellite remote sensing of the atmosphere (for example, control of the concentration of major greenhouse gases [19]). It requires taking into account not only the Doppler spectral line broadening associated with the thermal molecular motion, but also more subtle effects affecting the line shape near the resonance frequency, such as collisional line narrowing (Dicke effect) [20], the dependence of the collisional relaxation of molecules on their velocity (wind effect) [21], and the correlation between these effects, since both of them may result from the same collisions. The corresponding line shape model [22], referred to as HTP (Hartman - Tran Profile), has been recommended [23] by the International Union of Pure and Applied Chemistry (IUPAC) instead of the Voigt profile traditionally used in atmospheric spectroscopy applications.

1.2. Non-resonance absorption modeling

One of the most common ways to thermodynamically describe the non-ideality of gas that leads to the non-resonance absorption is the virial equation of state:

$$p = \frac{RT}{V_m}\left[1 + \frac{B(T)}{V_m} + \frac{C(T)}{V_m^2} + \cdots\right], \quad (7)$$

where p, R, V_m are pressure, universal gas constant, and molar volume, respectively, and B and C are the second and third virial coefficients, which are the functions of temperature T. In the case of an ideal gas, only unity is left in brackets in the right-hand side of the equation. The second virial coefficient takes into account all possible pair (binary) interactions of molecules with each other, the third one – triple interactions, and so on. Estimates show that even for pure water vapor (whose non-ideality is more pronounced in Earth's atmosphere than of any other major atmospheric gases) the simultaneous interaction between three or more molecules can be neglected (see, e.g. [24]). That is why the nature of the continuum absorption in Earth's atmosphere is considered to be the pair molecular (or bimolecular) absorption.

In [25] it was rigorously shown that $B(T)$ can be divided into parts corresponding to different states of molecular pairs. Three types of such states can be distinguished: (1) a state called free pairs, in which colliding molecules repel after a single approach; (2) a state, in which colliding molecules "stick" to each other to form double molecules (dimers) whose internal energy is greater than the dissociation energy of the pair, so that they can spontaneously split into two initial molecules; such a state is called metastable or quasi-bound dimers; (3) a state, in which the total internal energy of two bound molecules is less than the dissociation energy, called true bound or stable dimers. In accordance with this:

$$B(T) = B_f(T) + B_m(T) + B_b, \quad (8)$$

where B_f is responsible for the collision of free pairs of molecules, B_m takes into account the existence of metastable dimers (metadimers) in gas, and B_b – stable dimers.

It should be emphasized that this is only a general description of the collisional interaction between any two molecules. In air, which is a mixture of atmospheric gases, plenty of double molecules can result from a collision. If a pair is formed from identical molecules, such as, e.g. H_2O-H_2O, N_2-N_2, O_2-O_2, Ar-Ar, and CO_2-CO_2, then, accordingly, one speaks of the formation of a water dimer, nitrogen dimer, oxygen dimer, etc.; if different molecules are involved (H_2O-N_2, N_2-O_2, Ar-CO_2...), they are called heterodimers with corresponding names (for example, water-nitrogen heterodimer). At least two collisions are needed to form a stable dimer or a heterodimer. The metastable pair formed as a result of the first collision should transfer its excess energy to a third molecule to become stable. The stable pair may be formed only from a metastable pair as a result of successful collision. The answer to the question which state of a double molecule can be neglected under certain conditions (the main factor is temperature that determines the average energy of the collision) depends primarily on the properties of the monomer molecules constituting the pair (see ([26,27] and references therein). For example, in [26] it was shown that in pure water vapor at room temperature free pairs can be neglected, and the fractions of metastable and bound dimers are approximately the same. It is possible to talk about some common temperature-related behavior rules. Stable states always dominate at low temperatures, whereas free pairs – at high temperatures. The fraction of metastable states initially increases with increasing temperature due to the reduced number of stable states, and then decreases. Nonetheless, the temperatures characterizing these rules for different molecular pairs are very different. As an estimate for the steady state lifetime of a water metadimer that determines the characteristic line broadening in its spectrum, one can use the values of 0.3–0.8 ps [28] obtained from trajectory calculations. The lifetime of the metadimer itself is at least an order of magnitude larger and, in principle, can reach the time between collisions, which is determined by gas pressure.

The number of dimers formed in a gas under equilibrium conditions as a result of collisions is characterized by the dimerization constant

$$K = \frac{p_d}{p_m^2}, \tag{9}$$

where p_d and p_m are partial pressures of the dimers and monomers, respectively. The dimerization constant is a function of temperature.

It can easily be shown (see, e.g. [25]), that

$$B_b(T) = -K_b(T) \cdot RT, \quad B_m(T) = -K_m(T) \cdot RT, \quad B_f(T) = b_0, \tag{10}$$

where R is the universal gas constant, and b_0 is the so-called excluded volume introduced by Van der Waals to account for the repulsive intermolecular forces, which is also a function of temperature. The most accurate, to date, estimate of $b_0(T)$ based on the classical prerequisites for the equilibrium water vapor under near to atmospheric conditions can be found in [29]. The results of *ab initio* calculations of the dimerization constant for stable water dimers $K_b(T)$ were published in [30]. Experimental observations of the resolved rotational spectrum of water vapor dimers [31,32] confirmed the validity of these calculations to within multiplication of the derived dimerization constant by a factor of 0.65(6). (Here and further, value in brackets after the number stands for parameter error in units of the last given digit resulting from the optimization, which reflects the statistical error but usually does not account for possible systematic errors.) Such a decrease of the dimerization constant was expected and is associated with the overestimated value of dimer dissociation energy of 1232 cm^{-1} used in the *ab initio* calculations. Using instead the experimentally determined dimer dissociation energy of 1105(5) cm^{-1} [33] gives a coefficient of 0.54, which is in good agreement with the experimentally determined value of 0.65. To find the values of $B(T)$ in the temperature range from 273 to 1273 K, one can use the parameterization [24] based on the highly accurate empirical data [34]. Thus, the information accumulated so far allows estimation of the amount of water dimers formed in the atmosphere under various weather conditions. For example, under standard conditions (1 atm, 0 °C) and 50% humidity, partial pressures of stable dimers and metadimers of water vapor are, according to such estimates, about 0.4 and 0.2 mTorr, respectively.

For modeling of the water vapor non-resonance absorption, one needs to know the spectra of all pair states of water molecules. The spectrum of free pairs is calculated as the absorption occurring in monomers as a result of a short term transient collision-induced additional dipole moment (this absorption is sometimes referred to as the collision-induced absorption [28,35]). An example of such calculations for water vapor can be found in [36,37]. The most complete and rigorous calculations of the stable water dimer spectrum by modern quantum chemistry methods in the frequency range up to 600 cm^{-1} have been made in [38]. The spectrum of the dimer is so dense that at atmospheric pressure it completely merges into a smooth non-resonance absorption due to the collisional broadening of individual lines. For practical modeling of this spectrum in the millimeter wavelength range, the semi-empirical model proposed in [39] and the results of experimental observations [31,32] can be used. To assess the contribution of metadimers in the water vapor non-resonance absorption, two simplest models can be employed, which are based on the fact that the absorption cross-section of a metadimer must be greater than twice the cross-section of a monomer, but less than that of a stable dimer [40]. These models provide estimates for, respectively, the minimum and the maximum possible absorption by metadimers. In the first extreme case, the metadimer is considered as two monomers freely rotating near each other, and its spectrum is calculated as a doubled monomer spectrum whose lines are uniformly broadened by the short steady-state lifetime of metadimer (the half-width of lines 7–20 cm^{-1} [28]). In the second extreme case, the metadimer is considered indistinguishable in its structure from a stable dimer, and so its spectrum differs only by the spectral line width determined, as in the previous case, by its lifetime.

To model the non-resonance absorption of radiation in the atmosphere, it should be taken into account that bimolecular interactions and hence corresponding non-resonance absorption occur not only in pure water vapor, but also in any atmospheric gases and their mixtures. Thus, the non-resonance absorption spectrum for the general case should be calculated as

$$\alpha_{non\text{-}resonance} = \sum_{all\ pairs} \sum_{i} \left[C_i^{gas_1 - gas_2}(\nu, T) \cdot p_1 p_2 \right], \tag{11}$$

where the first summation over i yields the total spectrum of the aforementioned three pair states of the colliding molecules which may be identical or belong to different atmospheric gases 1 and 2, C_i is the spectra of corresponding pair states, and p_1 and p_2 are the partial pressures of these gases; the second summation is made over all possible pairs of atmospheric gases.

It has been experimentally established (see, e.g., review [41] and references therein) that the greatest contribution to the atmospheric non-resonance absorption is made by pair interactions of water molecules with each other and water molecules with molecules of other atmospheric gases (mainly determined by H_2O-O_2 and H_2O-N_2 molecular pairs). Almost everything is known for calculation of the pure water vapor non-resonance absorption spectrum, as described above, and it seems more or less real; as to the calculation of the heteromolecular component, only estimates of the equilibrium constants [42–45] and approximate calculations of the spectrum related to the H_20 and N_2 free pairs [46] are available so far.

Thus, despite the understanding of the physical nature, it is currently impossible to calculate the non-resonance absorption spectrum by formula (11). That is why the empirical models of this part of the total absorption are still used for atmospheric applications, which are based on laboratory and field measurements. This absorption is calculated following expression (2) as the difference between the total observed absorption and the calculated contribution of resonance lines. The result, however, contains the unknown contribution from far wings of atmospheric resonance lines at frequency detunings exceeding the maximum allowable one in the impact approximation (Section 1.1). To distinguish the result from the non-resonance absorption let us call it the continuum, which empirical definition is

$$\alpha_{continuum} = \alpha_{total} - \sum \alpha_{lines}. \tag{12}$$

The principal difference between this expression and expression (2) is that α_{total} is measured in experiment. After subtracting the calculated resonance lines (note that the choice of the line shape, its parameters and maximum frequency detuning begins to play a significant role as it directly affects the value of the resulting continuum), the obtained data are parameterized in some way. Given the dominant role of water vapor molecules in the formation of the atmospheric continuum and its bimolecular nature, the general expression for the continuum absorption coefficient, which follows from (11), can be represented as three terms corresponding to the interaction of water molecules with each other (quadratic continuum component with respect to humidity term), interaction between water molecules and air molecules (linear with respect to humidity term), and the interaction of dry air molecules with each other (dry continuum):

$$\alpha_{continuum}(\nu, T) = C_w(\nu, T) p_w^2 + C_{air}(\nu, T) p_{air} p_w + C_{dry}(\nu, T) p_{air}^2, \tag{13}$$

where p_w and p_{air} are the partial pressures of water vapor and dry air, respectively. It has been found experimentally [15,47–49] that in the millimeter wavelength range considered here, the continuum absorption is quadratically dependent on frequency, and its temperature dependence is satisfactorily described by a simple exponential function. This allows representing the expression (13) in the form

$$\alpha_{continuum}(\nu,T)=\left(C^0_w\left(\frac{T_0}{T}\right)^{x_w}p_w^2+C^0_{air}\left(\frac{T_0}{T}\right)^{x_{air}}p_{air}p_w+C^0_{dry}\left(\frac{T_0}{T}\right)^{x_{dry}}p_{air}^2\right)\cdot\nu^2, \quad (14)$$

where C^0_w, C^0_{air}, C^0_{dry}, x_{air}, x_w and x_{dry} are numerical coefficients. Note that in some studies (e.g. [16]), the factor $(T_0/T)^{-3}$ has been explicitly isolated in the parameterization of the continuum. This factor corresponds to the temperature dependence of the stimulated absorption by molecules, leading to a corresponding decrease in the temperature dependence exponents of all components of the continuum.

It's worth mentioning that Eq. (14) is also perfectly consistent with alternative representation of the continuum in mm wave range as cumulative contribution of far wings of distant resonance lines (see e.g. [50]). Indeed the resonance absorption at large detuning from the line center has quadratic dependence on frequency and its amplitude is in direct proportion to the product of the line width (linear depending on pressure of broadening gas) and concentration of absorbing molecules (linear depending on partial pressure of absorbers). This coincidence, on one hand, simplifies the problem of empirical modeling of the continuum. On the other hand, it makes more difficult to separate the bimolecular absorption from the observed continuum advancing towards physical model (2).

In summary of Section 1, let us briefly overview the theoretical aspects of absorption modeling, which have now been resolved with an accuracy sufficient for practical applications, and highlight those that require further consideration. The theoretical understanding of the resonance line shape near the line center (the frequency detuning range is ~10 widths) has been thoroughly elaborated. The physical mechanisms affecting the line shape in this region are well understood, and appropriate models have been developed. First-principles calculations of the line shape can be used to test the models. There are methods for calculating collision parameters of lines and their temperature dependences, the accuracy of which is close to the accuracy of modern experiments [51]. Still unsolved is the problem of the far line wings (frequency detuning about the duration of the collision), which appear to be associated with the continuum despite the fact that they are caused by resonance interaction of radiation with monomers. The nature of the components of the continuum absorption is theoretically understood within the bimolecular approximation. From this, in particular, there follows an obvious dependence of this absorption on partial pressures of gaseous constituents. There are no sufficiently accurate theoretical models for calculating spectra of the continuum components (especially in gas mixtures) and their temperature dependences. Therefore, parameters of the observed continuum are determined using empirical models, which have not been supported by accurate theoretical calculations and are based on experimental data only.

2. Parameters for modeling the atmospheric water vapor absorption

2.1. Parameters of the shape of the main diagnostic lines

In the frequency range from 20 to 300 GHz, the traditional frequency range for shortwave atmospheric radiometry, according to the HITRAN database, there are more than 50 water vapor resonance lines whose intensity allows their investigation in laboratory. Only two of them, however, are intense enough for radiometric analysis of atmospheric water. These are lines corresponding to the transitions within ground vibrational and electronic state with change in the rotational quantum numbers $J'_{Ka'Kc'} \leftarrow J_{KaKc} = 6_{16} \leftarrow 5_{23}$ at frequency near 22 GHz and $3_{13} \leftarrow 2_{20}$ at frequency near 183 GHz. In a higher frequency range, which is now being actively explored by radiometric methods, there is a huge number of water vapor lines, many of which are more intense, but all of them are much less studied than the above two lines, due to the historical inaccessibility of this frequency range. The four subsections to follow will provide a brief overview of all currently known studies relevant to the parameters of each of these lines.

2.1.1. Water vapor line near 22 GHz

The existence of water vapor absorption line near the frequency of 0.78 cm^{-1} (23.3 GHz) was theoretically predicted in the first half of the last century based on measurements of rotational spectral lines in the infrared range (see [52] and references therein).

The first experimental study of this line was performed due to the development of high-power sources in the 1-cm wavelength range for airborne and marine radars. It was found that the sensitivity of the radar operating at certain frequencies is highly dependent on weather conditions, particularly, on humidity. This appeared to be because the radar frequency coincides with the atmospheric water line. Radiation sources, relevant waveguides and other auxiliary tools were put at the disposal of researchers. Using equipment of this kind, the absorption of atmospheric air was carefully measured under laboratory conditions at 45 °C and strongly differing (from 10 to 50 g/m^3) humidity levels in the frequency range from 17 to 40 GHz [9]. A high-Q (Q ~ 700,000) cavity resonator (also called an "echo box", though it would be more correct to call it a "room", as the polished-copper walls of this "box" were about 2.5 m). The absorption was determined from the decay time of the radiation power inside the resonator. The huge by spectroscopic standards radiation power, as well as careful preparation and performance of the experiments provided a very high, even by modern standards, quality of the spectroscopic data.

Fig. 1 shows a comparison of the data obtained in [9] at a humidity of 30 g/m^3 with the result of absorption calculation using the modern version of MPM (Millimeterwave Propagation Model), which is one of the most popular propagation models for this wavelength range [15,53–55].

An invaluable advantage of this study is that not only values of the determined spectral line parameters were published, but also results of the absorption measurements. This allows to process them taking into account the constantly emerging new, more

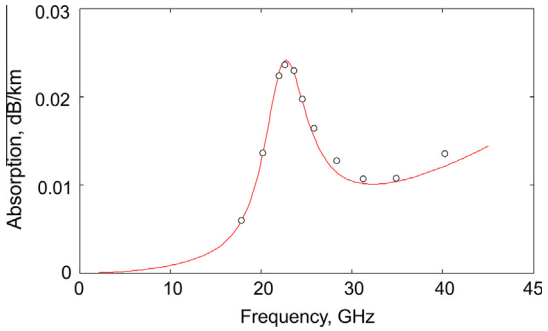

Fig. 1. Results of laboratory measurements [9] of radiation absorption in the humid air (pressure of 760 Torr, humidity of 30 g/m^3, temperature 45 °C) in the vicinity of the 22-GHz line (circles) and the result of calculation using the modern version of MPM (solid line).

accurate data on the spectrum of atmospheric air in order to refine the parameters of the line and the continuum in this spectral region. The results of this study have led to the above-mentioned conclusion about the proper shape of the atmospheric lines [8]. In this work, prior to extracting the line parameters from experimental data, a small systematic distortion of the 22-GHz line profile associated with the change in the broadening coefficient of the 60-GHz atmospheric oxygen band lines with changing humidity was considered. To calculate the correction to the experimental data, MPM and data from [56] were used. Line parameters after the data correction were determined as described in [9].

The frequency of the observed line center averaged over all experimental recordings was defined as 0.743(2) cm^{-1} (22.28(6) GHz, which within the statistical error coincides with the value 22235079.85(5) kHz measured in [57] by the Lamb dip method. The frequency of the observed center coincides in all recordings within the statistical error. However, there is its systematic (almost linear) decrease with increasing humidity, which corresponds to the self-shift parameter $\delta_w = -1.61(14)$ MHz/Torr.

The line width in the experimental conditions, according to Eq. (5), is composed of self-broadening and air-broadening. The total gas pressure and gas humidity were controlled in the experiment, allowing to unambiguously determine the broadening parameters $\gamma_w = 16.13(39)$ and $\gamma_a = 3.49(2)$ MHz/Torr. The comparison of these parameters with data from other studies will be done in Section 3.

The line intensity averaged over all experimental spectra and normalized to the concentration of water molecules was 4.41 $(10) \cdot 10^{-25}$ cm/mol, which is only 3% higher than the current HITRAN value (recalculated to 45 °C using formula (4)) and is consistent with it within 3σ.

Also in 1946, another study of the 22-GHz line was carried out, using a classical video spectrometer [58]. The temperature of vapor under study also was 45 °C. The line center frequency was measured as 22.235(5) GHz, and the self-broadening parameter was estimated to be $\gamma_w = 14.1$ MHz/Torr.

Another thorough investigation of the line parameters was undertaken more than 20 years later [59,60]. A classical resonator spectrometer based on a high-Q Fabry – Perot cavity filled with the gas being studied was used. The absorption value was determined by changes in the refractive index using the Kramers – Kronig relations. The absorption was investigated at a temperature of 27 °C in pure water vapor [59] and in a mixture with all major atmospheric gases, including He and CO_2 [60], which is important for accurate calculation of the air-broadened line parameter. The result of the integrated line intensity measurement was 13.92 ± 2% Hz/Torr = $4.226(85) \cdot 10^{-25}$ cm/mol. The zero pressure line center frequency was determined to be 22 235.15(1) MHz. The measured parameter of self-shifting of the line frequency $\delta_w = -1.38$ MHz/Torr is in good agreement with the result [9] mentioned above. The values of the collision broadening parameters measured in these experiments were $\gamma_w = 17.99(18)$ and $\gamma_a = 3.751(19)$ MHz/Torr. The value of γ_a was calculated from the measured in [60] parameters of pressure broadening by nitrogen, oxygen, argon and CO_2, taking into account their abundance in the atmosphere. It should be noted that applying the widely used simplified expression $\gamma_a = 0.21\gamma_{O2} + 0.79\gamma_{N2}$ in the calculations yields an error of about 0.5%, which corresponds to the maximum statistical error of determining the broadening parameter reported in [60].

Also worth mentioning is the study of broadening parameters of this line through the time of collisional relaxation of polarization induced in gas at low (up to 0.1 Torr) pressures [61]. The authors determined the pressure broadening parameter by water vapor $\gamma_w = 13.9(7)$ MHz/Torr at 20 °C and nitrogen $\gamma_{N2} = 4.14(50)$ at 22 °C.

The results of the most recent laboratory study of collisional parameters of the 22-GHz line, also performed at low (up to 0.15 Torr) pressures, were published in [62]. In this study, a classical video spectrometer with a high-accuracy frequency synthesizer was used. The measurements were carried out at three temperatures, 296.7, 318.9 and 337.9 K, allowing to estimate the temperature dependence of the line parameters. The Voigt profile was used. The frequency of the observed line center, in contrast to the previous studies in which resonator spectrometers were employed [9,59], almost linearly increased with increasing water vapor pressure in the range of 10–130 mTorr (approximately 30 measurements), giving the self-shifting parameter of $\delta_w = +0.84$ (10) MHz/Torr. The authors mention that the pressure shifting by nitrogen and consequently by air is lower than the measurement error. The non-shifted line center frequency of 22235.072(10) MHz, obtained from the experimental data, is in good agreement with the high-precision measurements [57]. The parameters of pressure broadening by water vapor and air[1] and their temperature dependences (Eq. (6)) are determined from the obtained data as $\gamma_w(296) = 16.67(21)$ MHz/Torr, $n_w = 1.23(54)$ and $\gamma_a(296) = 3.431$ (56) MHz/Torr, $n_a = 0.76(45)$, respectively. Note that the quantity 2σ is given as an error, which presumably takes into account possible systematic errors.

2.1.2. Water vapor line near 183 GHz

The existence of the water vapor absorption line near 6 cm^{-1} also followed from IR spectral measurements [52]. The line frequency (6.15 cm^{-1}) and intensity were approximately calculated in [63]. Interestingly, recalculating the found intensity taking into account the exact transition frequency yields a value of $7.894 \cdot 10^{-23}$ cm/mol, which is only 1.1% higher than the current HITRAN value. The first experimental observation of this line took place almost 10 years later than of the 22-GHz line, and was made using a classical video spectrometer with a harmonic generator [64]. As a result, an approximate value of the absorption coefficient was confirmed, and the line center frequency was found to be 183311.30(30) MHz.

The first experimental study of the collisional parameters of the 183-GHz line was also performed using a video spectrometer at low pressures (5–400 mTorr) and a temperature of 300 K [65]. The center frequency of the line was verified to be 183310.12 (10) MHz, the self-broadening parameter was defined $\gamma_w = 19.06$ (20) MHz/Torr, as well as broadening parameters by most abundant atmospheric gases (up to CO_2 including), allowing to determine the parameter γ_a as 3.526(46) MHz/Torr. A possible systematic measurement error was estimated by the author as 5%.

The first study of the 183-GHz line parameters using a resonator spectrometer was made in pure water vapor and in a mixture with nitrogen, oxygen and carbon dioxide at up to atmospheric pressures at a temperature of about 300 K [66]. The absorption coefficient in this spectrometer was determined at the eigenmode frequency of oscillations in an open Fabry - Perot resonator by changes in its Q factor occurring when the resonator was filled with absorbing gas. Available sources of coherent radiation and the design of the spectrometer resonator allowing slight changes in its length made it possible, in principle, to measure the gas absorption coefficient at certain points of the 100–300 GHz band. How the measurement data (Fig. 6 in [66]) correspond to contemporary models can be judged by comparing them with MPM calculation (Fig. 2).

To measure the line broadening parameter, the authors [66] measured in more detail the absorption at different frequency detunings from the line center ranging from −200 to +300 MHz. For data analysis, the following model function was used. The contours of the studied line and the adjacent absorption line at

[1] The air-broadening parameter was determined from measured parameters of pressure broadening by nitrogen and oxygen as $0.21\gamma_{O2} + 0.79\gamma_{N2}$.

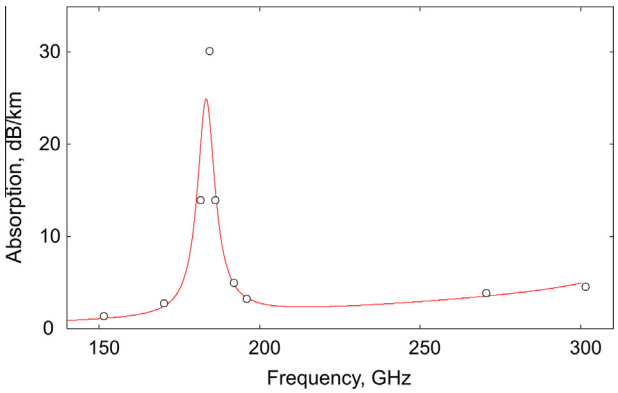

Fig. 2. Results of laboratory measurements of absorption [66] in humid nitrogen in the vicinity of 183 GHz line (points) and the result of calculation of the absorption under experimental conditions (nitrogen pressure 760 Torr, water vapor pressure 7.5 Torr, temperature 300 K) using MPM (considering the change in the model parameters when dry air is replaced by pure nitrogen).

325 GHz (its width was assumed to be the same as of the 183-GHz line) were modeled by the Van Vleck - Weisskopf profile. An additive purely quadratic term was used accounting for far wings of other lines. The intensities of both the lines were fixed on calculated values obtained from [63]. As a result, the broadening coefficients were found to be $\gamma_w = 22(2)$, $\gamma_{N2} = 4.4(2)$ and $\gamma_{O2} = 2.7(2)$ MHz/Torr. The estimated line broadening by dry air from these data is $0.21\gamma_{O2} + 0.79\gamma_{N2} = 4.04(20)$ MHz/Torr.

In [67] the 183-GHz line was studied in calibrated mixtures of water vapor with nitrogen and oxygen at four temperatures ranging from 242 to 325 K. The classical video spectrometer with a frequency doubler of frequency-unstabilized klystron and a superheterodyne receiver was used. Collisional broadening measurements were made in two regimes: (a) by continuously recording the line at pressures up to 5 Torr, and (b) by measuring the absorption at certain points at pressures ranging from 200 Torr (Fig. 3) to atmospheric pressure. In both the cases, at the same temperatures the authors obtained values that almost coincide with each other.

To consider the self-broadening contribution, values $\gamma_w = 19.1$ - MHz/Torr [65] and $n_w = 1$ were used. As a result, the authors yielded $\gamma_{N2}(300) = 3.54$ MHz/Torr, $n_{N2} = 0.74$. From measurements of oxygen broadening reported in the article and air broadening values calculated as $0.21\gamma_{O2} + 0.79\gamma_{N2}$ it follows that $\gamma_{O2}(300) = 2.80$ MHz/Torr, $n_{O2} = 3.37$ and $\gamma_a(300) = 3.39$ MHz/Torr, $n_a = 1.23$. The statistical error of the measurement results is a few percent. The authors do note, however, that the temperature dependence of the oxygen broadening is too strong, apparently due to an unknown systematic measurement error.

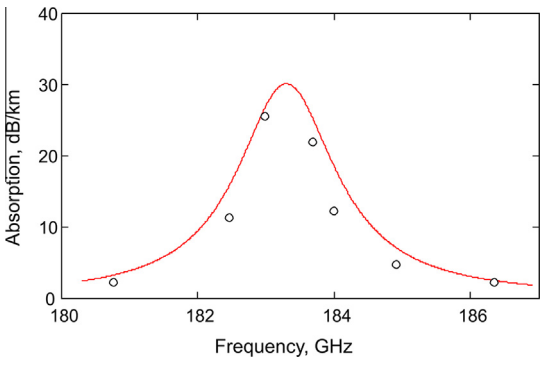

Fig. 3. Comparison of measurement results from [67] (points) with calculations using MPM (solid line). Total pressure of $H_2O + N_2$ mixture is 200 Torr, humidity 2.55 g/m^3, temperature 301.5 K.

Next in chronology is the study of the 183-GHz line parameters [68] conducted at room temperature (293–299 K) using approximately the same video spectrometer as in the previous study. The parameters of self-broadening and broadening by nitrogen were measured at pressures up to atmospheric. The observed line was approximated by the kinetic Zhevakin - Naumov profile [69] also known as the Gross profile [70]. The contribution from the wings of neighboring lines and the continuum was not considered. The line intensity was fixed on calculated value. The found parameters ($\gamma_w = 21.7(39)$ and $\gamma_{N2} = 4.38(20)$) are in good agreement with data from [66].

In another study [71], an attempt was made to evaluate the temperature dependence of parameters γ_w and γ_a. The video spectrometer with a harmonic generator was also used in this study, but the frequency of the primary radiation source was stabilized against a harmonic of high-accuracy reference radio signal. The study was performed at pressures from 30 to 600 mTorr and four temperatures ranging from 251 to 299 K. The Voigt line shape was used for data processing. The obtained parameter values for self-broadening demonstrated the expected systematic decrease with increasing temperature in accordance with $\gamma_w(296) = 20.48$ (40) MHz/Torr, $n_w = 1.17(6)$. In case of the dry air broadening the temperature dependence of the obtained parameter values looks arbitrary. Therefore, it seems reasonable only to recalculate the data from all the experiments to temperature 296 K using the temperature exponent from more recent studies, for example, 0.68 (HITRAN) and to average them. This procedure gives $\gamma_a(296) = 4.20(21)$ MHz/Torr.

Several years later the same authors published results of a similar, though much more thorough experiment conducted with the same experimental equipment in a wider temperature range from 300 to 390 K [72]. In this study, the authors, instead of the dry air, separately used all major atmospheric constituents, to argon inclusive. Note that the results of almost all measurements are consistent, within the statistical error, with smooth dependencies (6). The obtained data allow calculating the air-broadening parameter and its temperature dependence $\gamma_a(300) = 3.729(59)$ MHz/Torr, $n_a = 0.64(10)$. The values of $\gamma_w(300) = 19.88(8)$ MHz/Torr and $n_w = 0.85(5)$ were obtained for self-broadening. In addition, the authors presented the results of measurement of the line central frequency at very low pressure 183310.074(15) MHz and reported observed pressure shift in pure water vapor estimated by them as less than +0.7 MHz/Torr, which was further confirmed by subsequent measurements [73].

Approximately at the same time, a similar study was carried out by other authors using a very similar experimental setup, but in a much wider temperature range from 80 to 600 K [74]. That of course greatly increased the accuracy of determining the temperature exponent. In this work, when studying the line broadening by oxygen, nitrogen, and helium, the authors experimentally demonstrated, for the first time, the applicability of Eq. (6) for the entire range of the atmospheric temperatures. The deviation of the experimental points from the smooth power-law dependence (6) was observed only at temperatures below 140 °C. The use of the obtained data for calculation[1] of the air-broadening parameter yields $\gamma_a(300) = 3.85(15)$ MHz/Torr, $n_a = 0.76(3)$.

Twenty years later a study was conducted [75] of the temperature dependence of the self-broadening of the 183-GHz line using a spectrometer with a frequency synthesizer based on a backward-wave oscillator tube (BWO) and with radio-acoustic detection of absorption (RAD spectrometer [76], its modern version is described in [77]). Measurements were made at four temperatures ranging from 266 to 376 K and pressures within 0.1–0.9 Torr. A good statistical fit of the experimental data to expected theoretical dependencies was demonstrated. The following parameters were obtained $\gamma_w(297) = 21.69(45)$ MHz/Torr and $n_w = 0.66(6)$.

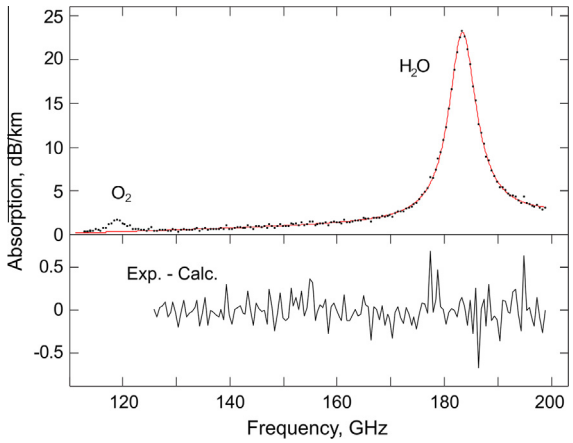

Fig. 4. Laboratory recording [78] of the atmospheric absorption spectrum around the 183-GHz line (dots) and the result of their approximation by the Van Vleck – Weisskopf profile with the addition of a quadratic-with-frequency polynomial accounting for contributions of adjacent line wings, continuum absorption and the baseline of the spectrometer. Residuals of the fit are shown in the lower part of the figure.

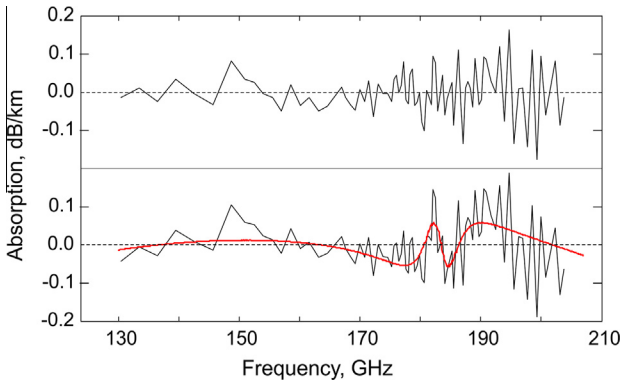

Fig. 5. Residuals of modeling atmospheric absorption spectrum recordings from [11]. Using the VanVleck – Weisskopf profile to consider absorption in the 183-GHz line gives the residual shown in the upper part of the figure, and the result of applying instead the complete Lorentz profile (Eq. (12) from [10]) is shown in the lower part. An additional quadratic-with-frequency polynomial is used in both cases to account for the continuum and the contribution of the resonance lines outside the frequency range. The smooth line in the lower part indicates a residual obtained if the VanVleck – Weisskopf profile is used for calculation of the absorption under experimental conditions and the Lorentz model is used for fitting. Note that the use of the Gross profile [70] gives exactly the same residuals as the Lorentz model. The root-mean-square deviation of the experimental points from the VanVleck – Weisskopf model (upper trace) is about 0.3% of the line amplitude. The amplitude of the systematic deviations of the points from either the Lorentz or Gross model (lower trace) reaches approximately the same value.

In 2000 the first continuous wide-range (113–200 GHz) highly sensitive recording of the absorption spectrum of laboratory air at atmospheric pressure (Fig. 4) performed with a resonator spectrometer of a new generation [78] confirmed the advantage of the Van Vleck - Weisskopf line shape for describing the resonance line profile at atmospheric pressure and allowed to determine the collisional air-broadening parameter of the 183 GHz line at 292.8 K as $\gamma_a = 3.985(40)$ MHz/Torr.

Results of a detailed study of the 183-GHz line using this spectrometer in a similarly wide range of frequencies in nitrogen, oxygen and air at atmospheric pressure, room temperature and various humidities were reported in [11]. The operating principle of the resonator spectrometer allows a direct (no additional calibration required) measurement of the absorption coefficient of a gas of interest. This allows the authors accurately measure the integrated intensity of the line, which at 297 K appeared to be $7.80(8) \cdot 10^{-23}$ cm/mol. The difference between this result and the current value from the HITRAN database is +0.8%. A better, compared to the previous study [78], signal-to-noise ratio on the spectrum recordings obtained in [11] clearly demonstrates that the 183-GHz line shape can be better modeled by the Van Vleck - Weisskopf profile (3) than by the Lorentz and Gross line shapes [70] (Fig. 5).

The first laboratory observation of the pressure shift of the line center frequency by air pressure $\delta_a = -67(16)$ kHz/Torr was also reported in [11]. Parameters of the collisional broadening were determined in this work as $\gamma_{N2}(299) = 4.24(4)$, $\gamma_{O2}(299) = 2.57(4)$ and $\gamma_a(298) = 3.84(4)$ MHz/Torr.

The results of the most recent laboratory investigation of collisional parameters of the considered line are presented in [73]. The study was performed with a modern version of RAD spectrometer at room temperature. All of the most abundant atmospheric constituents, including hydrogen and noble gases, were used as a broadening partner. The Voigt profile was employed for determining the parameters. In addition to the highly accurate (errors are fractions of a percent) determination of the broadening

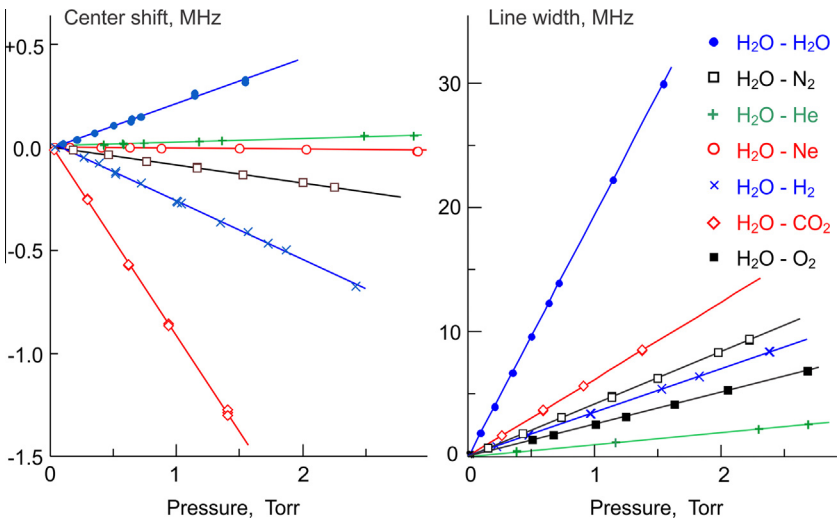

Fig. 6. Shifting of the 183-GHz line center frequency (left) and collisional width of the line (right) versus pressure for various atmospheric gases, according to the results of [73]. Points correspond to the experimental values (symbols representing various gases are shown in the legend at the right of the figure), and lines are the results of linear approximation.

parameters, systematic investigations of the shifting of the line center frequency by pressure of atmospheric gases were carried out in this study for the first time (Fig. 6).

The peculiarity of the study [73] was that experiments with different gases were conducted at temperatures differing within a few degrees. This slightly reduces the accuracy of the line parameters calculation for dry air because of the uncertainty in the temperature exponents, which in this case can give a recalculation error, comparable with the parameter error. Using values $n_{N2} = 0.74$, $n_{O2} = 0.85$ from [74] and approximated value $n = 0.7$ for other atmospheric gases provides, for the average temperature in these experiments, a broadening value of $\gamma_a(300) = 3.883(7)$ MHz/Torr and a shifting value of $\delta_a = -93(9)$ kHz/Torr.

2.1.3. Radiometric measurements

Experimental determination of the air broadening parameters of the lines discussed here should also include field measurements made directly in the atmosphere by the traditional spectrometric method with a light source and a detector located a large distance apart [79,80], as well as by using ground-based [81,82] and satellite-based [83] radiometers detecting thermal emission of the atmosphere.

The case of a near-surface horizontal path, the simplest case for analyzing retrieved data, was used in [79,80] to determine the 183-GHz line broadening.

The results of absorption measurements made during several summers on a about 6 km-long path above the sea surface have been reported in [79]. A BWO served as the light source, and a radiometer was the detector. The findings, together with similar data available at that time from other researchers, (Fig. 7) were analyzed using the Van Vleck – Weisskopf profile. As a result, the collisional line width was defined as 0.1025(35) cm^{-1}. The calculation of the dry-air broadening parameter requires taking into account the self-broadening contribution. Using the value of 19.5 MHz/Torr from [73] yields the air-broadening coefficient of $\gamma_a(300) = 3.88(14)$ MHz/Torr.

Results of similar measurements of the same line obtained with similar equipment but in autumn, at lower temperatures and lower humidity levels over a path length of 1.58 km have been reported in [80]. The measurement data were recalculated for average conditions of the experiments (284 K, 730 Torr, 10 g/m^3). To determine the line parameters, the authors used the Gross profile [70] and considered the self-broadening when calculating broadening by dry air. The resulting value is $\gamma_a(284) = 4.02(24)$ MHz/Torr.

More difficult to analyze and much more dependent on both the atmospheric absorption model and the model of the atmosphere itself are radiometric data obtained along limb paths and paths running vertically through the whole thickness of the atmosphere, as the received signal has contributions from all atmospheric layers with significantly differing thermodynamic conditions.

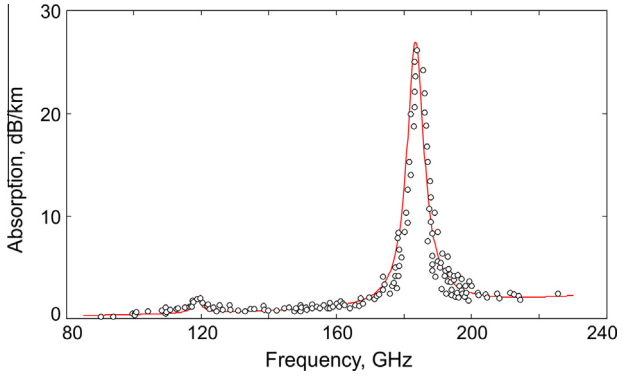

Fig. 7. Results of atmospheric absorption measurements along near-surface horizontal paths (according to Figs. 1 and 2 from [79]) for temperature 300 K, humidity 7.5 g/m^3 and pressure 760 Torr (circles) and the absorption modeling using the modern version of MPM (line).

The authors of [83] analyzed the atmospheric limb sounding data obtained from the URAS satellite (MLS radiometer) [84] and the ATLAS/MAS radiometer [85] operated on board the space shuttle, and demonstrated the possibility of determining the spectroscopic parameters of atmospheric diagnostic lines. In particular, for the 183-GHz line the best fit between the observed and calculated absorption profiles was obtained when the parameter of pressure-induced frequency shift of the line was introduced into the model. No laboratory measurements of this parameter had been previously reported, and the parameter had not been considered in any of the known propagation models. Assuming that $n_a = 0.75$ and $n_w = 1.38$, the authors [83] yield in MHz/Torr $\gamma_a(300) = 4.09(9)$, $\delta_a = -0.19(4)$ according to MLS data and $\gamma_a(300) = 4.6(2)$, $\delta_a = -0.27(5)$ according to MAS data. The authors note that the accuracy of MLS data is insufficient for reliable determination of the broadening parameter, but is sufficient to determine the shift.

There are two studies [81,82], in which the collisional broadening of the lines was determined from measurements of the atmospheric brightness temperature during zenith observation by ground-based radiometers. Here the results of only the more recent and more precise investigation [82] will be addressed, as the first study actually only demonstrated the possibility of such measurements in principle. For radiometric data processing, additional information about atmospheric temperature and humidity profiles retrieved by radiosondes, and the radiative transfer model MonoRTM [16] were used. The parameters γ_a for the 22-GHz and 183-GHz lines, included in the model, were varied to achieve the best possible fit to measurement results. Values $\gamma_a(296) = 3.60(11)$ MHz/Torr and $n_a = 0.755$ for the 22-GHz line, and $\gamma_a(296) = 3.93(12)$ MHz/Torr and $n_a = 0.769$ for the 183-GHz line were used as initial values of the parameters for model optimization and in order to account for their temperature dependence. These values were calculated by the most accurate to date method [86]. The end results of [82] are values $\gamma_a(296) = 3.550(57)$ and 3.913(63) MHz/Torr for the 22-GHz and 183-GHz lines, respectively.

2.1.4. Measurement of relevant vib-rotational lines

Another source of experimental information about the collisional broadening of the lines discussed here can be spectral measurements of vibration-rotational lines of water vapor in the infrared range. This is due to the well-known fact that relaxation of rotational states of molecules prevails during molecular collision. A detailed analysis of this fact has been made for H_2O molecule in [87,88]. It has been shown that at least for lower vibrational states, a marked difference of the line broadening parameters from parameters of corresponding lines of purely rotational spectrum should manifest itself only at large values of the quantum number J, corresponding to the total angular momentum of the molecule. Thus, the collisional broadening parameters should be approximately the same (maximum possible deviation of less than a few percent) for the lines of all water-molecule transitions occurring between rotational levels with the same quantum numbers J, K_a, K_c, as for the lines discussed here in the ground vibrational state and excited vibrational states, including the fundamental modes and their first overtones. Moreover, the spectral lines corresponding to the same type of transitions of various isotopologues of the molecule are also identically broadened by pressure [89,90]. This means that our comparative analysis may also include the results of studies [91–95], in which the broadband vibrational-rotational spectra of pure water vapor and in a mixture with major atmospheric gases were studied using Fourier spectrometers.

Table 1
Vibrational-rotational transitions of H_2O analog for the 22-GHz line.

Vibrational transition	Oxygen isotop	ν_0, cm^{-1}	γ_a, MHz/Torr	n_a	γ_w, MHz/Torr	Reference
020–010	16	1547.8901	–	–	16.698(8)	[91]
020–010	16	1584.1688	–	–	17.05(26)	[91]
010–000	18	1589.2183	–	–	16.303(37)	[91]
010–000	16	1596.2426	–		17.36(60)	[91]
			3.72(31)	–	–	[92]
			3.657(18)	0.601(54)	17.27(71)	[95]
010–000	18	1600.5764	–	–	17.44(41)	[91]
010–000	16	1606.7163	–	–	17.74(41)	[91]
			3.64(31)	0.71(13)	–	[92]
			3.74(10)	–	–	[94]
			3.676(15)	0.664(50)	18.07(71)	[95]
200–000	16	7189.3444	3.949(79)	–	19.329(79)	[93]

Table 2
Vibrational-rotational transitions of H_2O analog for the 183-GHz line.

Vibrational transition	Oxygen isotop	ν_0, cm^{-1}	γ_a, MHz/Torr	n_a	γ_w, MHz/Torr	Reference
020–010	16	1556.5047	–	–	16.993(8)	[91]
010–000	18	1597.4797	–	–	17.61(54)	[91]
020–010	16	1577.7269	–	–	18.77(41)	[91]
010–000	18	1593.8697	–	–	16.57(14)	[91]
010–000	17	1600.2346	–		18.11(76)	[91]
010–000	16	1601.2079	–	–	18.00(51)	[91]
		1601.2079	3.90(22)	–	–	[92]
		1601.2079	3.89(12)	0.67(21)	–	[94]
		1601.2079	3.925(16)	0.777(32)	17.48(61)	[95]
010–000	16	1603.3198	3.92(15)	–	–	[92]
		1603.3198	3.99(12)	0.80(15)	–	[94]
		1603.3198	3.921(16)	0.680(32)	19.06(50)	[95]

Corresponding lines and their parameters are given in Table 1 and in Table 2 for the 22-GHz and the 183-GHz line analogs respectively.

The pressure-induced frequency shift of molecular line is, in contrast, strongly dependent on the vibrational state of the molecule [87], and therefore the comparison is not applicable in this case.

2.2. Parameters of the continuum

The study of the continuum is a much more complex and time-consuming task than that of the resonance lines. The problem consists of many factors acting simultaneously, which magnifies the complexity of the measurements. The most significant of these factors are (a) small value of continuum absorption, (b) weak frequency and strong temperature dependences, and (c) the need for accurately subtracting the resonance absorption contribution from the total absorption. As a result, systematic laboratory studies of the humidity-related atmospheric continuum in the millimeter - submillimeter wavelength range have been undertaken so far by only a few research groups at the Institute for Telecommunication Sciences, USA, the University of Lille, France, Ohio University, USA, and the historically interrelated Radiophysical Research Institute (RRI) and Institute of Applied Physics (IAP RAS), Russia. In most cases, resonator spectrometers were utilized in the measurements, as most suitable for such investigations in the mm and submm range. Only the research team from RRI used a multi-pass cell in their research in the range, where the continuum absorption becomes quite strong as it grows quadratically with frequency. Field experiments performed on long near-surface horizontal paths [96,97] and with ground-based radiometers [98–100] have also made a significant contribution to the continuum parameters determination.

The first and perhaps most punctual was a series of investigations of the continuum performed at the Institute for Telecommunication Sciences by Hans Liebe (H.J. Liebe) in the 1970–1990s. The main goal was to develop a propagation model for millimeter waves in the atmosphere. The description of the spectrometer and preliminary results of the continuum measurements can be found in [47]. It was mentioned therein that the spectrometer could operate in the frequency range from 30 to 300 GHz. However, judging by publications, actual measurements with this spectrometer were made only in the 60-GHz range (oxygen absorption) and near 138 GHz (absorption measurements in the atmospheric transparency window to define the continuum parameters). Detailed results of the study of the absorption in the transparency window were reported in [101]. The majority of the absorption measurements (around 2500 data points) were made in pure water vapor and its mixtures with the atmospheric air at six temperatures ranging from 282 to 316 K, pressures up to 1.5 atmospheres and relative gas humidity from 0 to 95%. In addition, at a temperature of 303 K additional absorption measurements were conducted in mixtures of water vapor with oxygen (at pressures up to 2.4 atm, which made it possible to determine, among all, parameters of the dry continuum), nitrogen, and argon. After subtracting the contribution of resonance lines the results of these measurements allowed to define all numerical parameters of the continuum (14). Major results of this study are shown in Fig. 8.

The next extensive series of investigations aimed at clarifying the physical nature of the continuum was undertaken at the Lille University in the 1985–2002 [48,102–110]. The description of the spectrometer can be found in [102]. Measurements were made at individual points at frequencies ranging from 157 GHz to 350 GHz (Fig. 9), temperatures from 296 to 360 K and atmospheric pressure. In most experiments, the absorption was measured in a mixture of water vapor and nitrogen at varying humidities. Only at 239 GHz additional measurements were carried out in mixtures

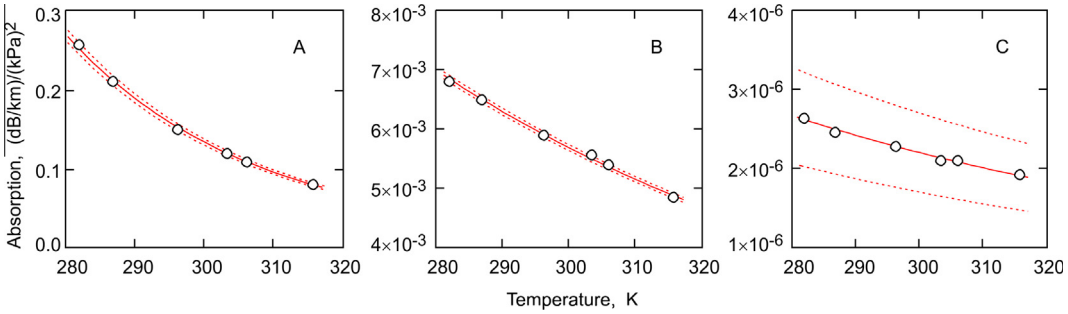

Fig. 8. Results of atmospheric absorption measurements at frequency 137.8 GHz [101]. Panels A, B and C show, respectively, quadratic-with-humidity, linear-with-humidity, and humidity-independent absorption components (terms of function (14)). Each point is the result of averaging over a large number of measurements. Solid lines show the result of approximation by corresponding terms of function (14). Dotted lines indicate the estimated error range.

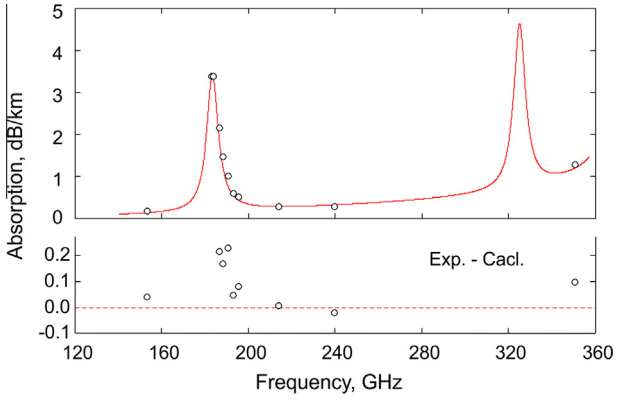

Fig. 9. Top panel - absorption measurements in a H_2O-N_2 mixture in a series of studies [48,102–106] (each point is the result of averaging over a series of measurements). The smooth curve corresponds to the model absorption under conditions of the experiments (a mixture of water vapor (1 Torr) with nitrogen (750 Torr) at a temperature of 23 °C) calculated using the modern MPM version. Bottom panel – the difference between measured and calculated absorption.

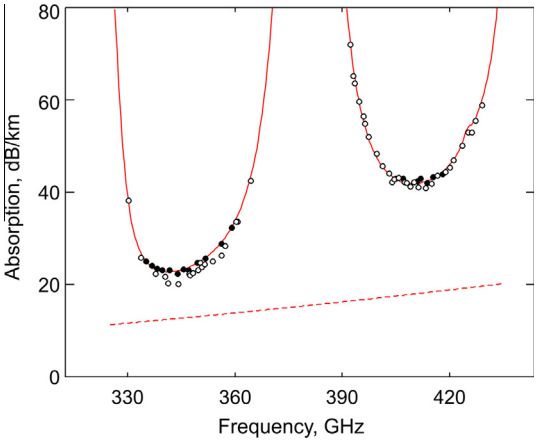

Fig. 10. Measurements of atmospheric absorption at dry air pressure of 735 Torr, humidity of 19 g/m^3 and temperature 306 K according to the results of [111,112]. Field measurements [111] are indicated by filled circles, laboratory measurements – open circles. MPM was used to re-calculate the data for the same weather conditions. The solid line shows calculation by the modern MPM version. The dashed line in the lower part of the figure corresponds to the continuum absorption calculated by MPM.

of water vapor and carbon dioxide (CO_2) [107,108], methane (CH_4) [109], ethylene (C_2H_4) and ethane (C_2H_6) [108]. Generalization of the results and an attempt of physical interpretation[2] of the observed continuum were given in [110]. The results of the absorption measurements in a mixture of water vapor with nitrogen related to the atmospheric continuum were generalized in [48]. Assuming that the quadratic dependence of the continuum absorption on frequency is maintained over the whole range of measurements, the authors took into account the contribution of the resonance lines and determined the continuum coefficients C_w, x_w, C_{N2} and x_{N2}.

From the early 1970s to the late 1990s, a research group from RRI investigated specific features of the mm/submm absorption in the atmospheric transparency windows. The results of their laboratory studies are presented in [111,112] and are shown in Fig. 10. The measurements were performed at room temperature, atmospheric pressure and varying air humidity levels under well-controlled conditions with the use of a multi-pass cell providing the total path length of ~140 m. The results of field measurements made by the same authors on a near-surface path of about 1 km are also given in the figure for comparison. In all cases, measurements were performed using the classical scheme of the video spectrometer. The light source was a BWO, and the detector was an optical-acoustic receiver (Golay cell). The authors reported only on the results of the absorption measurement and extraction the linear-with-humidity and quadratic-with-humidity components. The contributions of the resonance lines and the continuum were not separated.

The results of the extensive field measurements carried out by this research group with the aim to study the quadratic-with-humidity component of the continuum have been generalized in [96]. The absorption measurements are reported for atmospheric transparency windows at frequencies 138, 247, 260, 340 and 410 GHz in the temperature range from 270 to 310 K. Analysis of the data (taking into account the estimated contribution of the resonance lines and the linear-with-humidity component of the continuum[3] has allowed the authors to state that under conditions of their study the degree of the temperature dependence of the quadratic component of the continuum x_w does not exceed the limit of 10–15. The authors note that x_w decreases with increasing frequency. However, normalizing the obtained absorption to the square of the frequency leads to the conclusion that all the data are in good agreement with each other within the specified measurement errors (Fig. 11).

Results of a series of field measurements of the atmospheric absorption over a near-surface path 21.4 km in length in Alaska

[2] The authors erroneously attributed the observed continuum to collision-induced absorption, which was further criticized in [35].

[3] The difference between calculated values obtained by the authors (Table 2 of [96]) and similar data obtained by MPM does not exceed a few percent.

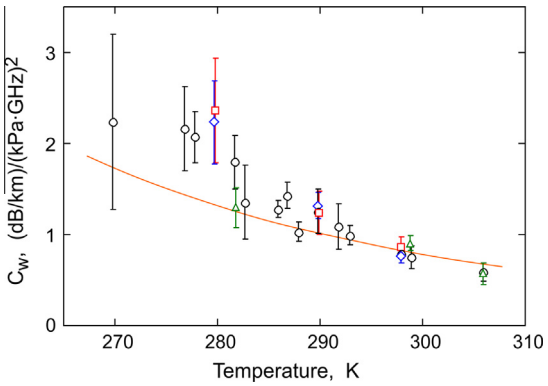

Fig. 11. Temperature dependence of the quadratic-with-humidity component of the continuum C_w according to Fig. 1 - 3 of [96]. Squares, diamonds, circles and triangles show measurement results at 138, 247, 340 and 410 GHz, respectively. Solid line indicates calculation by the modern MPM.

mountain region at temperatures ranging from 4 to 32 °C and humidity 3–21 g/m^3 have been reported in [97]. Measurements were performed at a frequency of 96.1 GHz using the classical video spectrometer scheme with a stabilized light source and a superheterodyne receiver. Periodic calibrations of the measurement equipment and active thermal stabilization of the transmitting and receiving electronics provided a baseline stability of less than 0.05 dB/km. The authors have not determined the continuum coefficients by their data, but have demonstrated a good agreement between the measurements and calculations with MPM-87 [101].

Studies of the atmospheric continuum using radiometers for detection of thermal emission of the atmosphere at vertical paths deserve a separate mention here. A specific feature of these measurements is the much stronger dependence of the measurement result on the absorption model used, as compared to radiometric measurements of the resonance lines parameters. The results of the most well-known measurements of the brightness temperature of the atmosphere thickness, obtained from ground-based zenith-pointing stations at the end of the last century, can be found in [98]. The measurements were performed at frequencies of 20.6, 31.65 and 90.0 GHz in different climatic zones, providing a wide range of atmospheric temperatures and humidities. Data analysis allowed the authors to evaluate the advantages of a particular model used for modeling thermal emission of the atmosphere under the observation conditions. These data helped to specify the continuum coefficients in MPM [15]. The obtained values of the coefficients are exploited in the model up to now. Examples of more recent similar studies of the continuum can be found in [99,100] and references therein. The broader capabilities of modern radiometric measurements allow the authors to improve the agreement between measurements and predictions by a particular model, by empirically introducing factors in the coefficients of the model continuum. It should be noted that the observed discrepancies could be caused not by the coefficient error but by some factors not considered in the model but affecting the measurement results. However, an indirect confirmation of the objectivity of the obtained data is that the introduction of coefficients to achieve the agreement between experiment and calculation in one transparency window leads to improvement of the agreement in another [99].

The most recent research of direct relevance to the atmospheric continuum in the mm wavelength range includes a series of measurements carried out using a resonator spectrometer of a new generation at the IAP RAS in wet nitrogen [49], pure water vapor [31,32] and a water vapor/air mixture [32]. The research is still underway. Its main distinctive feature is that two resonators having the same radiation field distribution but different lengths (differing by exactly a factor of two) are used simultaneously in the spectrometer. In its measurement principle, this method is equivalent to the variable-path length method, which is used in radiometry and excludes many systematic errors. In this spectrometer, the use of two resonators made it possible to eliminate the systematic error encountered in all previous laboratory measurements of the continuum. The error is associated with the adsorption of water molecules on mirrors and coupling elements of the resonator spectrometers (see for details [77]). The results of long-term systematic studies of the continuum in the range 107–143 GHz in wet nitrogen at atmospheric pressure, at temperatures ranging from 261 to 328 K (about one million individual absorption measurements) are reported in [49]. It was demonstrated that after subtracting the contribution of the resonance lines from the total observed absorption, the remaining continuum quadratically depends on frequency. Also, the linear- and quadratic-with-humidity components of the continuum were extracted (Fig. 12), and the values of coefficients C_w, C_{N2}, x_{N2}, and x_w were determined. A tendency is noted for the temperature exponent x_w to increase at decreasing temperature. This is consistent with the results of [26], from which it follows that at decreasing temperatures the fractions of metastable and bound dimers redistribute in favor of the latter, whose absorption is stronger dependent on temperature than the metastable dimer absorption.

The contribution of stable water dimers (H_2O-H_2O) to the continuum absorption of water vapor has been studied in [31,32]. It has been experimentally confirmed that the value of this contribution to the pure water vapor continuum is the same as to the continuum of atmospheric air at the same partial pressure of water vapor. The results of these experiments provide necessary

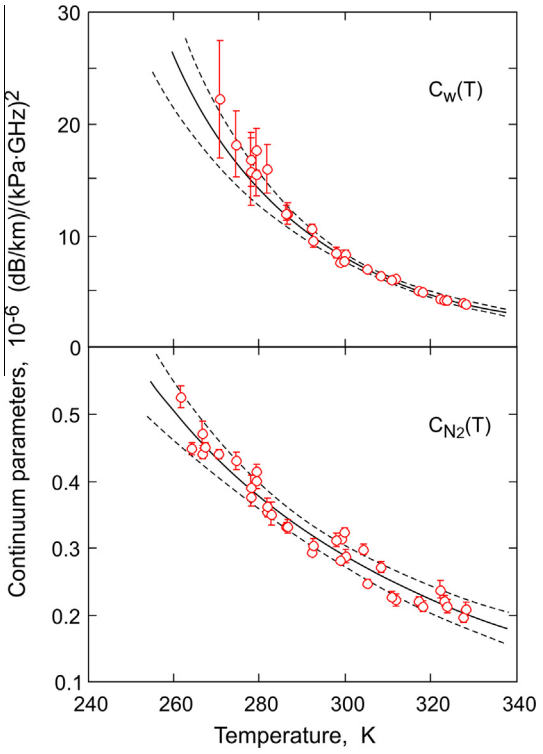

Fig. 12. Temperature dependences of wet nitrogen continuum coefficients from [49]. Each point is the result of separating the continuum spectrum obtained at a given temperature in the frequency range 107–143 GHz into quadratic and linear with humidity components. Vertical lines indicate the statistical errors of the measurement. Solid lines are the result of power function approximation of the points (14). Dashed lines are estimation of error in determining the continuum coefficients.

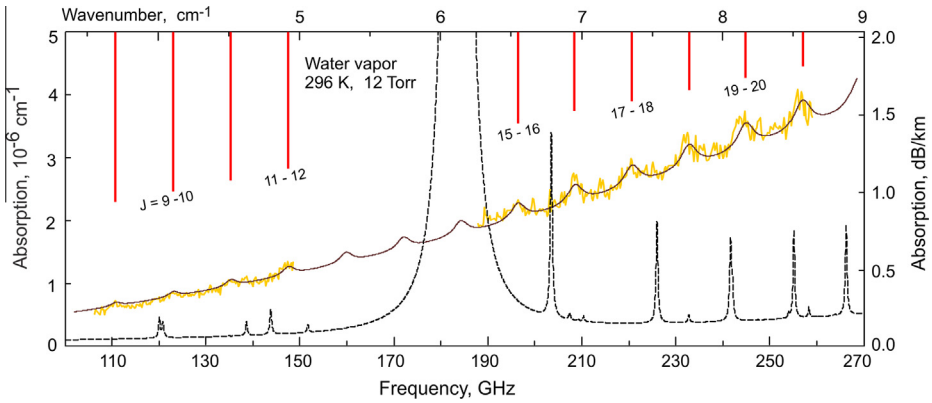

Fig. 13. Manifestation of the resolved rotational spectrum of water dimer in the continuum spectrum of pure water vapor according to the experimental results of [31,32]. Dashed line shows the calculated spectrum of the H_2O molecule. "Noisy" line corresponds to the measured total absorption, from which the calculated H_2O spectrum is subtracted. Vertical bars in the upper part indicate the positions of stable dimer lines corresponding to the successive transitions with a change in the value of the total angular momentum **J** (shown in the figure) as it rotates relative to the axis with the maximum momentum of inertia. Smooth curving line corresponds to the semi-empirical model of the dimer spectrum [39].

information to calculate the absorption of stable dimers of atmospheric water vapor in the temperature range typical for the Earth's atmosphere in the frequency range 60–300 GHz (Fig. 13) by a simple semi-empirical model [39].

For the sake of completeness, we should mention two more types of the atmospheric absorption that contribute to the total absorption at frequencies near the diagnostic lines of water vapor. These are (a) the absorption in atmospheric oxygen, which includes the resonant absorption in the spectral lines, and the so-called Debye absorption (see, e.g. [10]), which occurs due to the presence of the magnetic dipole moment in the oxygen molecules, and (b) the "dry" atmospheric continuum not related with humidity.

Information about modeling of oxygen absorption in the wavelength range considered here can be found in [54,55,113] and references therein.

When modeling the dry continuum, it should be kept in mind that almost all the continuum results from collisional interaction of molecules of atmospheric nitrogen and oxygen with each other. In atmospheric conditions, the contribution of the continuum to absorption in the wavelength range considered here is negligibly small, compared to other components of the non-resonance absorption (Fig. 8). However, taking it into account improves the description of experimental data (see, e.g. [114]). The most recent study devoted to the experimental investigation of all the major components of the dry atmospheric continuum is [115]. The coefficients of the continuum in pure nitrogen, oxygen and their 79/21 percent mixture were measured at various temperatures ranging from 230 to 320 K and pressures reaching up to 3 atmospheres. These results are consistent with previous measurements and theoretical calculations, and provide comprehensive information for the modeling of the dry continuum.

3. Discussion

The results overviewed in the previous section suggest that the deviation of the shape of the lines under consideration at atmospheric pressure from the model (3) does not exceed 0.3% of the line amplitude.

At low pressures no analysis of the air-broadened line shape has been made so far. However, a conclusion about the applicability of the Voigt profile for these lines can be drawn by analyzing recordings of the line in a mixture with nitrogen, as the most abundant constituent of the atmosphere. Examples of the 22-GHz line profile recordings at pressures ranging from 10 mTorr to 120 mTorr can be found in [116]. The signal-to-noise ratio in these recordings is more than 100, but the authors indicate the absence of any visible deviations of the observed line shape from the Voigt profile. The difference of the 183-GHz line shape from the Voigt profile at pressures from 0.1 to 1 Torr can be evaluated using data from [73]. It follows from these data that the deviations do not exceed 1% (Fig. 14). For a more precise modeling of the shape, one should use the HTP model [22,23]. Note that the use of this profile requires corresponding collisional parameters. The values of these parameters for the lines considered here have not been determined to date in either of the known studies. The parameters discussed in this paper are related only to the Voigt, Lorentz, Gross and Van Vleck - Weisskopf models.

3.1. Line profile parameters

Among the best-defined parameters of the line profiles discussed here are central frequencies (22235079.85(5) kHz [57] and 183310087(1) kHz [117]), and lower level energies (446.5106590(2) cm^{-1} and 136.163927(1) cm^{-1}, respectively

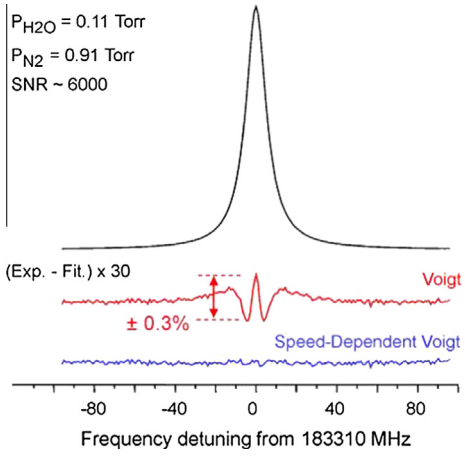

Fig. 14. Recording of the 183-GHz line in a mixture of H_2O with N_2 at room temperature using RAD spectrometer. Partial pressures of the gases in the mixture are shown in the figure. In the lower part are the residual of the line processing by the traditional Voigt profile and the Voigt profile taking into account the dependence of the collisional cross-section of molecules on their velocities, known as "wing effect" (qSDVoigt profile).

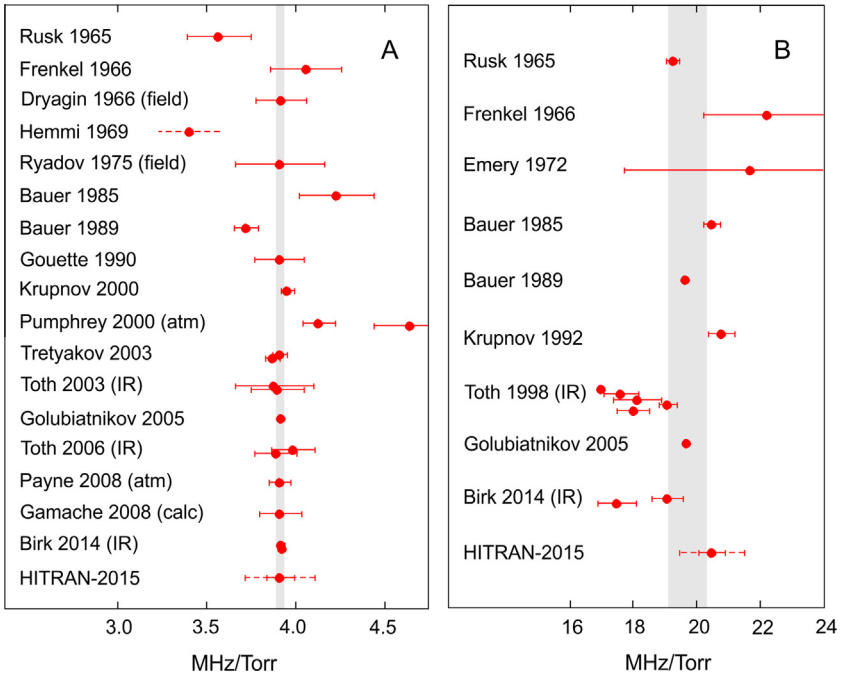

Fig. 15. The collisional broadening parameter of the 183-GHz line by pressure of dry air (panel A) and pure water vapor (panel B) at 296 K according to the results of various studies, in chronological order. The shaded area corresponds to the estimate of the parameter value made in this paper based on the analysis of available data (see text).

[118]), which were determined from the frequencies of the observed lines corresponding to all transitions which include these levels. Their integral intensity calculated in [119] based on the most accurate, to date, dipole moment surface of the water molecule [120] at 296 K and 100% concentration of the absorbing molecules is $4.390 \cdot 10^{-25}$ and $7.746 \cdot 10^{-23}$ cm/mol for the 22-GHz and 183-GHz line, respectively. The intensities are given with the allowance for corrections resulting from the replacement of the *ab initio* line frequencies used in the calculations [119] by the aforementioned experimental line frequencies. The authors evaluated the relative accuracy of their calculations for these lines as 0.3–0.5%. The obtained values are 0.35 and 0.77% lower than the corresponding intensities from the HITRAN-2015 database,[4] which are derived from calculations that take into account a large number of measurements of the lines of different vibration-rotational bands. This and the agreement between the above-mentioned measurements of the 183-GHz line intensity [11] with calculated data suggest that for practical applications it is possible to use the above values of line intensities, assuming that their error is less than 1%. Note that the 22-GHz line intensity measurements were less accurate. Results of the only two studies [9,60] are, respectively, 3% higher and 3.5% lower than the value given in the current HITRAN database. Note that in the first case obtained value is consistent with HITRAN within 3σ statistical error but in the second one the difference is almost twice larger than estimated 2-% uncertainty. It should be kept in mind that recalculating line intensities using Eq. (4) one does not take into account the change of the molecular partition function with temperature. However, for atmospheric conditions this change is practically negligible. For example, temperature variation from 296 down to 196 K leads to the relative change of the partition function of about 0.016%.

A comparative analysis of the broadening parameters of the lines of interest obtained by different researchers requires bringing all the data to the same conditions. Primarily, this means recalculation of the parameter values at the temperature at which they were measured to the temperature of 296 K, the common temperature for the most atmospheric databases, using Eq. (6). In this study, the values of $n_w = 0.78$ (weighted average from [72,75] for both lines), $n_a = 0.76$ or 0.77 (for the 22- and 183-GHz lines, respectively [82]), $n_{N2} = 0.74$ and $n_{O2} = 0.85$ from [74] were used for the recalculation. The uncertainty of these data has a negligibly small effect on the recalculation result. In case of determining the broadening/shifting parameter by dry air, it is also necessary to take into account the contribution of self-broadening/self-shifting, which not always was properly taken into account or was even neglected by the authors. During recalculation, we used the values of the parameters from [73]. In cases where the air-broadening parameter was defined as the sum of components corresponding to atmospheric gases, there could occur the above-mentioned systematic error associated with the insufficient adequacy of the dry air model. The evaluation of this error and the value of the correction coefficient for the 183-GHz line can be obtained based on the results of [73] and known concentrations of gaseous constituents of the Earth's atmosphere. Assuming a zero error of the air-broadening parameter calculated by the model (0.78084 N_2 + 0.209476 O_2 + 0.00934 Ar + 0.000314 CO_2 + 0.00003 Ne), one can find that the systematic relative broadening error calculated according to the simplified model (0.781 N_2 + 0.209 O_2 + 0.0096 Ar + 0.0004 CO_2) is + 0.012%. The use of model (0.78 N_2 + 0.21 O_2 + 0.01 Ar) gives an error −0.07%, and the most widely used model (0.79 N_2 + 0.21 O_2) overestimates the broadening by 0.5%.

The recalculated results of all the known from publications measurements of the collisional broadening parameters of the discussed lines in pure water vapor (self-broadening parameter γ_w) and in air (parameter γ_a) are shown in Figs. 15 and 16.

Similar diagrams for the temperature dependence exponents n_w and n_a of the lines discussed here are shown in Fig. 17. Note that the temperature dependence of the self-broadening of the 22-GHz line was measured only in one study [62]. The uncertainty of the obtained value $n_w = 1.23(54)$ is 44%.

[4] When comparing data it should be kept in mind that in the HITRAN the line intensities include the factor 0.9973, corresponding to the natural abundance of $H_2{}^{16}O$ isotopologue.

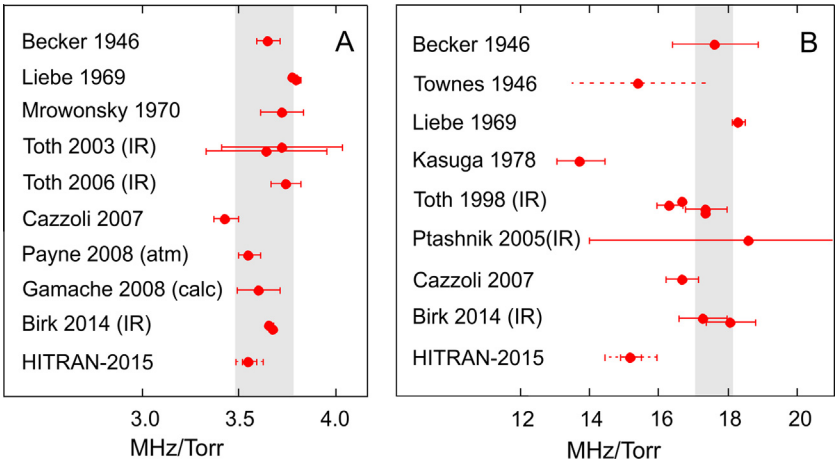

Fig. 16. The collisional broadening parameter of the 22-GHz line by pressure of dry air (panel A) and pure water vapor (Panel B) at 296 K according to the results of various studies, in chronological order. The shaded area corresponds to the estimate of the parameter made in this paper based on the analysis of available data (see text).

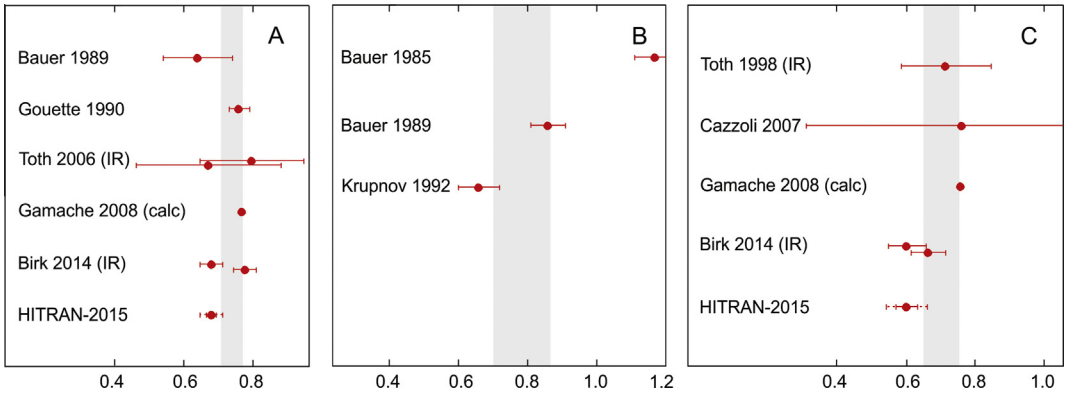

Fig. 17. Temperature dependence exponents of the collisional broadening of the 183 GHz line (panel A – air-broadening, panel B – self-broadening) and of the 22 GHz line (panel C – air-broadening) according to the results of various studies, in chronological order. The shaded area corresponds to the estimate of the parameter value made in this paper (see text).

Less data are available on the pressure shifting parameter than on the broadening parameter of the lines discussed here, and their temperature dependences have not been investigated. To evaluate the n_δ parameter one can use, for example, approximate theoretical considerations given in [121]. They imply that the temperature dependence of the shifting parameter is related to the temperature dependence of broadening as $n_\delta \sim 1.5n_\gamma + 0.25$. This means that if n_γ is within the range from 0.6 to 0.8 (Fig. 17), n_δ should be in the range 1.15–1.45. Given the qualitative nature of this approach and absence of experimental data we suggest using temperature dependences of the broadening parameter n_γ as an estimate of unknown temperature dependences of the shifting parameters n_δ. All known data about the shifting parameters of the lines recalculated to 296 K are summarized in Table 3.

Figs. 15–17 and Table 3 obviously demonstrate the problem of unknown systematic measurement errors discussed in many previous studies. The results of even most careful investigations may differ from each other, going significantly beyond the limits of measurement error range. The problem arises from the fact that authors usually give only the statistical error that corresponds to the spread of the obtained values with respect to the model used by the authors. The most common sources of the systematic error may be: (a) Uncontrolled changes of the spectrometer baseline when gas being studied is injected, which are connected both with the change in the refractive index of the medium through which the radiation passes and with mechanical changes of the optical path length of the spectrometer due to pressure drops or temperature drifts; (b) Inadequacy of the model used to describe the initial experimental data to these data; (c) Calibration error of measuring instruments; (d) When working with water vapor, the worst controllable sources of systematic errors are the processes of absorption and desorption of water molecules by spectrometer elements, which can lead to changes in the partial pressure of water vapor, as well as to changes in the output signal of the spectrometer [47,77,122].

Table 3
Line center linear with pressure frequency shifting coefficients for the 22- and 183-GHz lines.

Line	δ_w, MHz/Torr	δ_a, MHz/Torr	$n_{\delta a}$	Reference
22 GHz	−1.61(14)			[9]
	−1.40			[59]
	+0.82(10)	+0.02(50)[a]	2.6(20)[a]	[62]
		−0.035		[82]
		−0.032(39[b])		HITRAN [19]
183 GHz	less than +0.7			[72]
		−0.19(4)		MAS [83]
		−0.27(5)		MLS [83]
		−0.069(16)		[11]
	+0.23(3)	−0.096(10)		[73]
		−0.106		[82]
		−0.106(39[b])		HITRAN [19]

[a] Estimated from data reported by authors.
[b] The uncertainty interval estimation is 0.039–0.39 MHz/Torr.

That is why multiple measurements under different experimental conditions using instruments based on different principles are believed to be required for determining a reliable value of the parameter (see, for example, overview articles [87,123]). If fast yet reliable results are needed, the best choice is to use an instrumental complex of one research group. A good example is the complex of [124], which was repeatedly employed to study parameters of the atmospheric diagnostic lines [31,55,125–130]. It includes a resonator spectrometer [77], whose working pressure range corresponds to the near-surface atmospheric layers, and a spectrometer with radio-acoustic absorption detection (RAD spectrometer) [131] allowing investigations to be carried out at pressures ranging from tens of milliTorr to a few Torr, which corresponds to pressures in the upper layers of the atmosphere. An example of using this system for measuring pressure-induced broadening and shifting parameters of the 183-GHz diagnostic line is shown in Fig. 18. The coincidence of the measurement results within statistical errors means that the systematic errors are minimized in both the spectrometers comprising the complex. Such measurements significantly increase the reliability of determining the line parameters. Recently, the capabilities of this system were expanded by adding a video spectrometer [132] that can operate at pressures close to the interstellar medium. The confirmation of the high measurement accuracy of the system can be found in Fig. 15A, showing that subsequent measurements did not lead to further refinement of the parameter value.

Analysis of the measurement results shown in Figs. 15–17 and in Table 3, taking into account the measurement errors reported by the authors and the probabilities of possible systematic errors, allows to find best estimates of spectroscopic parameters of the water vapor lines considered here, which would provide the best fit of the proposed absorption model to the available data, and to evaluate the uncertainty of these parameters (Table 4). It should be noted that the presented values are the result of an expert assessment made by the author of this review and are subjective, to a large extent.

For comparison, Figs. 15–17 and Table 3 show current values of corresponding parameters and their uncertainties from the HITRAN database, whose popularity is maintained by regularly adding new and updating existing information. These data are actually also the result of subjective expert judgment of database creators. In almost all cases, with the exception of the 22-GHz line self-broadening, the parameter value estimation in this overview coincides with HITRAN within uncertainty limits, but in most cases HITRAN error estimates are more conservative.

3.2. Parameters of the continuum

A detailed analysis of a series of laboratory data obtained by Liebe [47,101] and Bauer [104–106] on the atmospheric continuum absorption in the cm-mm wavelength range can be found in [15,133]. The analysis was performed in order to select such coefficients of the humidity-related atmospheric continuum model (13) and (14) that would provide the best agreement between calculated absorption and radiometric data. This paper presents a similar analysis of the same data, updated by the more recent

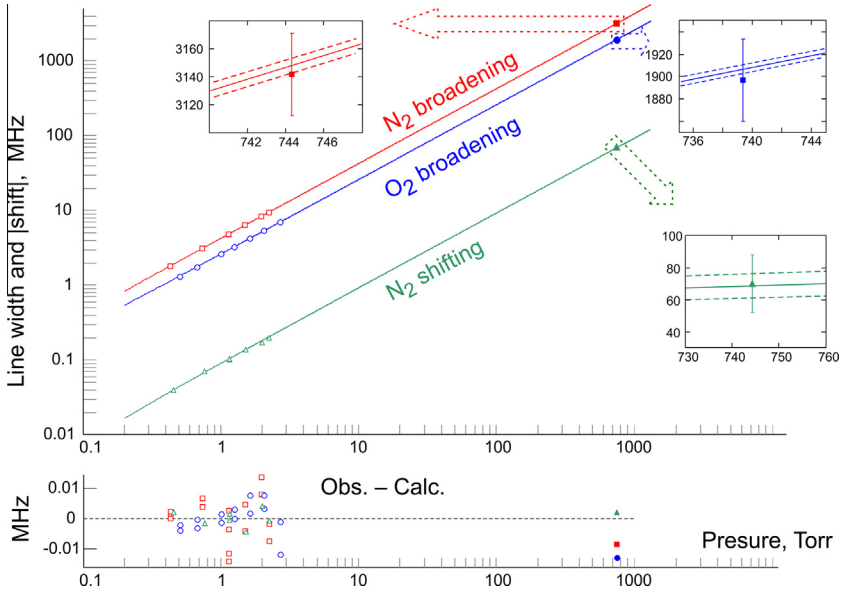

Fig. 18. The broadening and the shift modulus (line frequency shift induced by nitrogen pressure is negative) of the 183-GHz line by pressure of major atmospheric gases, according to the results of measurements by the spectrometric complex [124]. Solid lines correspond to the approximation of measurement results using a RAD spectrometer [73] (open symbols) extrapolated to the working pressure range of the resonator spectrometer. The deviation of the measurement results obtained by the resonator spectrometer (filled symbols) [11] from the extrapolation is shown in the insets on an enlarged scale. Dotted lines in the insets correspond to the statistical uncertainty of the RAD spectrometer data. Vertical lines in the insets indicate the statistical error of the resonator data. The deviation of experimental points from lines is shown in the lower part of the figure.

Table 4
Spectroscopic parameters of the 22- and 183-GHz lines at 296 K assuming the Voigt profile.

Transition $J'_{Ka'Kc'} \leftarrow J_{KaKc}$	ν_0, kHz	S^a, 10^{-25} cm/mol	E_{low}, cm^{-1}	γ_a, MHz/Torr	γ_w, MHz/Torr	δ_a, MHz/Torr	δ_w, MHz/Torr	n_a	n_w
$6_{16} \leftarrow 5_{23}$	22,235,079.85(5)	4.390(43)	446.5106590(2)	3.63(14)	17.6(5)	0.0(1)	−0.4(12)	0.70(5)	1.2(5)
$3_{13} \leftarrow 2_{20}$	183,310,087(1)	774.6(77)	136.163927(1)	3.926(20)	19.7(5)	−0.96(10)	+0.23(3)	0.74(3)	0.78(8)

[a] Intensity is given taking into account natural abundance of $H_2^{16}O$ isotopologue (99.73(3)%) in accordance with HITRAN's convention.

series of laboratory studies [48,49], and by the results of field measurements on a near-surface path [96].

The results of all mentioned in Section 2.2 measurements of the continuum C_w and C_{air} at different temperatures are shown in Fig. 19, which are analogous to Figs. 2 and 5 of [15,133], respectively. The common factor $(300/T)^3$ is used for the convenience of comparing with [15]. The use of a logarithmic scale in the construction of Fig. 19 allows to judge about the applicability of using the simplest power approximation for the temperature dependence of the continuum spectrum.

Despite the considerable scattering of the experimental points (30–50% for the quadratic part and 20–30% for linear) from the absorption value at a given temperature, it can be seen that different measurement series agree well with each other. Of particular note is the good agreement between the most accurate laboratory data on the quadratic component of the continuum [49] and data obtained in the field conditions over a long-distance near-surface path [96]. At room temperature, all measurements give almost the same value of absorption. Solid lines in the figure correspond to the modern MPM. Their parameters were chosen in [15] as a result of a compromise fit of the continuum model (14) to laboratory and radiometric measurements. The MRM functions do not look alien in Fig. 19, even taking into account the new experimental data [48,49,96]. On the contrary, at above-room temperatures one can speak about good agreement. At below-room temperatures all measurement results are above the model. Moreover, the laboratory data [49] supported by field measurements [96] suggest the impossibility of describing the quadratic component of the atmospheric continuum by power function (14). According to these data, the temperature exponent x_w in the temperature range of 300–330 K is 8.1(3) (which is very close to the MPM's value of 7.5), and in the range of 270–300 K, it is equal to 10.6 (6). This within error limits coincides with a value of 10.67, which corresponds to the temperature dependence of absorption of mm-waves by stable dimers of atmospheric water vapor, according to the most accurate to date quantum chemical calculations [38]. Such a change in the degree of temperature dependence of the continuum is justified by the fact that the absorption of stable dimers dominates over other types of bimolecular absorption at low temperatures, but becomes small at high temperatures [26]. Laboratory data [48,49] are also indicative of a stronger than MPM growth of the linear-with-humidity component of the continuum with decreasing temperature. In order to understand whether the corresponding change of the continuum coefficients in MPM will result in a more precise description of the radiometric data, let's have a look at the results reported in [99]. It has been demonstrated that the introduction of factors 0.79(18) and 1.11(10), respectively, into the quadratic and linear components of the continuum in MPM (dotted lines in Fig. 19) significantly improves the agreement between the calculations of the brightness temperature of the atmospheric column and the results of zenith-pointing radiometry. The decrease of one continuum component in the absorption model is compensated by a corresponding increase of the other. The brightness temperature of the atmosphere with such correction remains approximately constant over a wide range of air humidity. The correction of MPM based on measurements [49] requires a simultaneous increase of both the linear and quadratic with humidity components of the continuum, which, in view of the foregoing, will obviously lead to an increase of the total absorption and a systematic discrepancy between the calculated and measured brightness temperatures. The converse also holds: the comparison of the results of MPM correction based on radiometric data in the zenith direction with laboratory and field measurements on near-earth paths reveals a worse fit to the model, which is particularly noticeable in the quadratic component (Fig. 19) where the discrepancy goes beyond the uncertainty limits and becomes unacceptable.

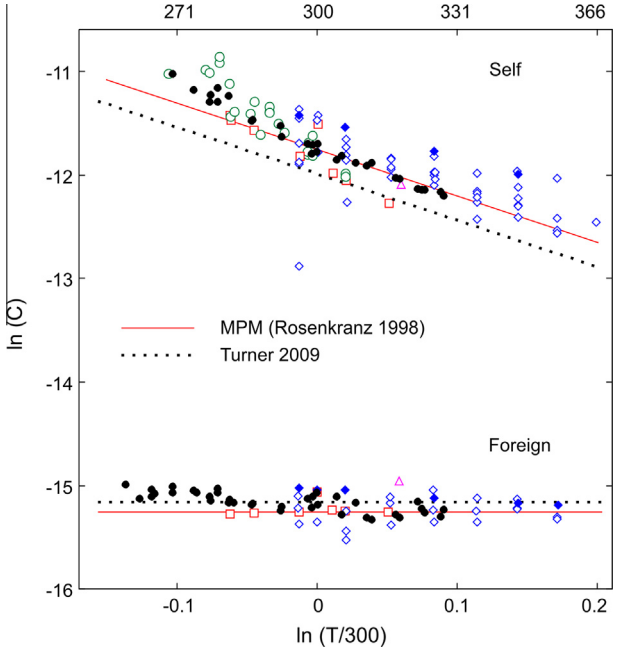

Fig. 19. Experimental data on the temperature dependence of the quadratic (top) and linear (bottom) with humidity components of the atmospheric continuum. Open diamonds are the results of a series of studies conducted by Bauer et al. [104–106]; squares - Libe et al. [47,101] (how these points correspond to different frequencies and measurement conditions can be found in [15]); triangle – Becker and Autler [9]; filled diamonds - Kuhn et al. [48]; circles – Katkov et al. [96]; points – Koshelev et al. [49]. Solid lines correspond to the modern MPM model. Dotted lines - MPM correction by radiometric data [99]. Units of C_w are (dB/km)/(GHz·kPa)^2, T is in Kelvin (upper scale).

Radiometric measurements in the zenith made by different researchers in different places using different equipment under strongly differing atmospheric conditions are consistent with each other. The general agreement between the different laboratory and field measurements can be seen in Fig. 19. It is currently impossible to match these two different methods of studying the atmospheric absorption using a common absorption model. This suggests that the source of the problem is not possible systematic errors of the experiments, but rather the uncertainty of the atmospheric air model, including the insufficient accuracy of describing the distribution of thermodynamic parameters and concentration of absorbing molecules with height. The development of such a model requires new theoretical and experimental efforts and goes far beyond the scope of this paper.

Summarizing, it can be said that within the framework of the existing atmospheric model the parameters of the humidity-related continuum from the current MPM version [15] seem to be the most adequate compromise. These parameters are given in Table 5. The empirical definition of the continuum (12) implies that these parameters should be used together with exactly the same algorithm of calculating the resonance absorption. Even if the lineshape parameters are updated, then the continuum coefficients may need some tweaking to be consistent with them.

Table 5
Coefficient of the atmospheric continuum approximation function (14) for the millimeter-wave range in (dB/km)/(kPa·GHz)^2 at $T_0 = 300$ K in accordance with [15,115].

C_w^0	x_w	C_{air}^0	x_{air}	C_{dry}^0	x_{dry}
$7.82 \cdot 10^{-6}$	7.5	$2.36 \cdot 10^{-7}$	3	$3.18 \cdot 10^{-11}$	3.35

One can estimate the limits of accuracy in the description of radiometric data with such a set of parameters from Fig. 6 of [15]. The figure shows the difference between the measured and calculated brightness temperature of the atmosphere in case of zenith observations over a wide humidity range. The continuum parameters for calculations were taken from the current MPM model (solid lines in Fig. 19). The scatter of experimental points over the whole range is about 6 K. So, it can be seen that at low and high humidity levels the calculation, on average, is in good agreement with experiment. At moderate humidities, there is a systematic excess, by about 2 K, of calculated temperature over experimental one.

4. Conclusions and recommendations

The comparison of the results of investigations of the diagnostic lines discussed here (Figs. 15–17 and Tables 3 and 4) suggests that currently almost all parameters of the 183-GHz line are known more accurately than those of the 22-GHz line. An exception is the central frequency of the 22-GHz line, whose relative error is about twice as small. The probable error of intensities of both the lines is about the same - less than one percent, but the estimated value for the 183-GHz line has been checked experimentally.

Estimates of the impact of the parameter error of the resonance spectral lines of atmospheric gases on the recovery of concentration of respective absorbers based on satellite remote sensing data have been made, for example, in [134]. They suggest, in particular, that (a) the relative intensity error is included in the relative concentration error with a weight close to 1; (b) the influence of the central frequency error is negligible; (c) the dominant error is associated with the uncertainty of the line air-broadening parameter and the uncertainty of the temperature dependence of the broadening, and (d) uncertainties of the parameters of pressure-induced self-broadening and shifting are exhibited to a much lesser degree. The most important, from this viewpoint, parameter of air broadening is known about an order of magnitude more accurately for the 183-GHz line than for the 22-GHz line.

It is obvious that errors of other components of the atmospheric absorption at the diagnostic line frequencies will also lead to the concentration recovery error. The contributions may be from (a) the resonance absorption in the far wings of other water vapor lines, (b) the absorption in atmospheric oxygen, and (c) the atmospheric continuum absorption. All these mechanisms near the diagnostic lines form an absorption that slowly varies with frequency. The relative contribution of errors of these absorption components to the water vapor concentration recovery error should be proportional to the ratio of this absorption to the resonance absorption of water molecules at the frequency of the diagnostic line. Estimates of corresponding absorptions made with the use of MPM suggest the following conclusions: (a) the relative contribution of the far wings of other water vapor resonance lines at the frequencies of both the diagnostic lines is practically the same and amounts to less than 1%. (b) The fraction of the oxygen absorption at 183 GHz is negligibly small. It increases with decreasing humidity, but even at low humidities corresponding to a height of about 6 km it remains less than 1%, while at 22 GHz it is about 80% under the same conditions. (c) The relative contribution of the continuum at 183 GHz for various meteorological parameters is systematically from 1.5 to 3 times smaller than at 22.2 GHz, although in both the cases the continuum absorption is only a few percent of the absorption in the line center almost for all conditions of the atmosphere. These estimates point to the advantages of the 183-GHz line for remote monitoring of atmospheric humidity.

It should be noted that in terms of readiness to use and availability of modern microwave equipment the 22-GHz and 183-GHz frequencies are practically identical. However, high-precision experimental investigations of the 22-GHz line parameters and the continuum in the line area are technically more sophisticated and much more time and cost consuming than for the 183-GHz line. The main difficulty is associated with more severe manifestations of the interference of the longer-wavelength radiation. The second factor is the more than two orders of magnitude difference in the line intensity lines. To have the same signal-to-noise ratio on spectral recordings, the spectrometer for the 22-GHz line should be two orders of magnitude more sensitive than for the 183-GHz line. When choosing between the two diagnostic lines, one should also consider the inevitable need to refine the spectroscopic parameters as technical capabilities of radiometry advance.

In conclusion, it is worth noting some specific features of the modeling associated with the humidity-related absorption in various layers of the atmosphere. In cold and rarefied upper layers of the stratosphere, the major interfering factor may be the poorly understood disturbance of the thermodynamic equilibrium of water vapor associated with the atmospheric chemistry, which results in a mismatch between the table and actual line intensities. The narrow resonance lines of minor atmospheric constituents can fall into frequency channels of radiometers, and therefore should be taken into account. In the line shape modeling, it is necessary to consider not only the Doppler component of the line broadening, but the poorly-studied collisional narrowing (known as the Dicke effect) as well. Additional collisional broadening associated with ionospheric plasma may also have some impact. In warm, dense and moisture-saturated near-surface layer of the atmosphere, the resonance line profile and its parameters are determined with greater accuracy than in the upper layers, though the accuracy of the modeling can be further improved by taking into account the dependence of the collisional relaxation of molecules on their velocity (wind effect). Of great importance in these conditions are the far wings of water vapor lines, the wings of adjacent H_2O and O_2 lines, the atmospheric continuum and, in particular, its quadratic-with-humidity component associated with the water vapor dimer absorption.

Acknowledgements

The author thanks P.W. Rosenkranz and two unknown reviewers for careful reading the manuscript and valuable comments improving its quality. This work was partially supported by the Russian Foundation for Fundamental Research.

References

[1] J.T. Kiehl, K.E. Trenberth, Bull. Am. Meteorol. Soc. 78 (1997) 197–208.
[2] K.E. Trenberth, J.T. Fasullo, J. Kiehl, Bull. Am. Met. Soc. 90 (2009) 311–324.
[3] I.M. Held, B.J. Soden, Annu. Rev. Energy Environ. 25 (2000) 441–475.
[4] B. Stevens, S. Bony, Phys. Today 66 (2013) 29–34.
[5] J.H. Jiang, H. Su, C. Zhai, V.S. Perun, A.D. Genio, L.S. Nazarenko, L.J. Donner, L. Horowitz, C. Seman, J. Cole, A. Gettelman, M.A. Ringer, L. Rotstayn, S. Jeffrey, T. Wu, F. Brient, J.-L. Dufresne, H. Kawai, T. Koshiro, M. Watanabe, T.S. Lecuyer, E.M. Volodin, T. Iversen, H. Drange, M.D.S. Mesquita, W.G. Read, J.W. Waters, B. Tian, J. Teixeira, G.L. Stephens, J. Geophys. Res. 117 (2012) D14105.
[6] H. Brogniez, G. Clain, R. Roca, J. App, Meteorol. Climatol. 54 (2015) 896–908.
[7] M.I. Hegglin, D.A. Plummer, T.G. Shepherd, J.F. Scinocca, J. Anderson, L. Froidevaux, B. Funke, D. Hurst, A. Rozanov, J. Urban, T. von Clarmann, K.A. Walker, H.J. Wang, S. Tegtmeier, K. Weigel, Nat. Geosci. 7 (2014) 768–776.
[8] R.J. Hill, Radio Sci. 21 (1986) 447–451.
[9] G.E. Becker, S.H. Autler, Phys. Rev. 70 (1946) 300–307.
[10] J.H. Van Vleck, V.F. Weisskopf, Rev. Mod. Phys. 17 (1945) 227–236.
[11] M.Yu. Tretyakov, V.V. Parshin, M.A. Koshelev, V.N. Shanin, S.E. Myasnikova, A. F. Krupnov, J. Mol. Spectr. 218 (2003) 239–245.
[12] D.M. Slocum, R.H. Giles, T.M. Goyette, J. Quant. Spectrosc. Radiat. Transfer 156 (2015) 69–79.

[13] S.A. Clough, F.X. Kneizys, R.W. Davies, R. Gamache, R.H. Tipping, in: A. Deepak, T.D. Wilkerson, L.H. Ruhnke (Eds.), Atmospheric Water Vapor, U.K. Academic, London, 1980, pp. 25–46.
[14] S.A. Clough, F.X. Kneizys, R.W. Davies, Atmos. Res. 23 (1989) 229–241.
[15] P.W. Rosenkranz, Radio Sci. 33 (1998) 919–928.
[16] S.A. Clough, M.W. Shephard, E. Mlawer, J.S. Delamere, M. Iacono, K.E. Cady-Pereira, S. Boukabara, P.D. Brown, J. Quant. Spectrosc. Radiat. Transfer 91 (2005) 233–244.
[17] C.H. Townes, A.L. Schawlow, Microwave Spectroscopy, McGraw-Hill, NY, 1955.
[18] L.S. Rothman, I.E. Gordon, Y. Babikov, A. Barbe, D.C. Benner, P.F. Bernath, M. Birk, L. Bizzocchi, V. Boudon, L.R. Brown, A. Campargue, K. Chance, E.A. Cohen, L.H. Coudert, V.M. Devi, B.J. Drouin, A. Fayt, J.-M. Flaud, R.R. Gamache, J.J. Harrison, J.-M. Hartmann, C. Hill, J.T. Hodges, D. Jacquemart, A. Jolly, J. Lamouroux, R.J. Le Roy, G. Li, D.A. Long, O.M. Lyulin, C.J. Mackiea, S.T. Massies, S. Mikhailenko, H.S.P. Müller, O.V. Naumenko, A.V. Nikitin, J. Orphal, V. Perevalov, A. Perrin, E.R. Polovtseva, C. Richard, M.A.H. Smith, E. Starikova, K. Sung, S. Tashkun, J. Tennyson, G.C. Toon, Vl.G. Tyuterev, G. Wagner, J. Quant. Spectrosc. Radiat. Transfer 130 (2013) 4–50.
[19] J.J. Harrison, P.F. Bernath, G. Kirchengast, J. Quant. Spectrosc. Radiat. Transfer 112 (2011) 2347–2354.
[20] R.H. Dicke, Phys. Rev. 89 (1953) 472–473.
[21] J. Berman, J. Quant. Spectrosc. Radiat. Transfer 12 (1972) 1331–1342.
[22] N.H. Ngo, D. Lisak, H. Tran, J.-M. Hartmann, J. Quant. Spectrosc. Radiat. Transfer 129 (2013) 89–100.
[23] J. Tennyson, P.F. Bernath, A. Campargue, A.G. Csaszar, L. Daumont, R.R. Gamache, J.T. Hodges, D. Lisak, O.V. Naumenko, L.S. Rothman, H. Tran, N.F. Zobov, J. Buldyreva, C.D. Boone, M.D. De Vizia, L. Gianfrani, J.M. Hartmann, R. McPheat, D. Weidmann, J. Murray, N.H. Ngo, O.L. Polyansky, Pure Appl. Chem. 86 (2014) 1931–1943.
[24] M.Yu. Tretyakov, E.A. Serov, T.A. Odintsova, Radiophys. Quantum Electron. 54 (2012) 700–716.
[25] D.E. Storgyn, J.O. Hirschfelder, J. Chem. Phys. 31 (1959) 1531–1545.
[26] A.A. Vigasin, Infrared Phys. 32 (1991) 461–470.
[27] A.A. Vigasin, in: C. Camy-Peyret, A.A. Vigasin (Eds.), Weakly Interacting Molecular Pairs: Unconventional Absorbers of Radiation in the Atmosphere, Kluwer Academic Publishers, Netherlands, 2003, pp. 23–47.
[28] I.V. Ptashnik, K.P. Shine, A.A. Vigasin, J. Quant. Spectrosc. Radiat. Transfer 112 (2011) 1286–1303.
[29] C. Leforestier, J. Chem. Phys. 40 (2014) 074106.
[30] Y. Scribano, N. Goldman, R.J. Saykally, C. Leforestier, J. Phys. Chem. A 110 (2006) 5411–5419.
[31] M.Yu. Tretyakov, E.A. Serov, M.A. Koshelev, V.V. Parshin, A.F. Krupnov, Phys. Rev. Lett. 110 (2013) 093001.
[32] E.A. Serov, M.A. Koshelev, T.A. Odintsova, V.V. Parshin, M.Yu. Tretyakov, Phys. Chem. Chem. Phys. 47 (2014) 26221–26233.
[33] B.E. Rocher-Casterline, L.C. Ch'ng, A.K. Mollner, H. Reisler, J. Chem. Phys. 134 (2011) 211101.
[34] W. Wagner, A. Pruss, J. Phys. Chem. Ref. Data 31 (2002) 387–535.
[35] A.A. Vigasin, J. Quant. Spectrosc. Radiat. Transfer 148 (2014) 58–64.
[36] C. Leforestier, R.H. Tipping, Q. Ma, J. Chem. Phys. 132 (2010) 164302.
[37] M.Yu. Tretyakov, A.A. Sisoev, T.A. Odintsova, A.A. Kyuberis, Radiophys. Quantum Electron. 58 (2015) 262–276.
[38] Y. Scribano, C. Leforestier, J. Chem. Phys. 126 (2007) 234301.
[39] T.A. Odintsova, M.Yu. Tretyakov, A.F. Krupnov, C. Leforestier, J. Quant. Spectr. Radiat. Transfer 140 (2014) 75–80.
[40] A.A. Vigasin, Mol. Phys. 108 (2010) 2309–2313.
[41] K.P. Shine, I.V. Ptashnik, G. Rädel, Surv. Geophys. 33 (2012) 535–555.
[42] I.M. Svishchev, R.J. Boyd, J. Phys. Chem. A 102 (1998) 7294–7296.
[43] T.W. Robinson, H.G. Kjaergaard, J. Chem. Phys. 117 (2003) 3717–3720.
[44] V. Vaida, J.E. Headrik, J. Phys. Chem. 104 (2000) 5401–5412.
[45] A. Sabu, S. Kondo, R. Saito, Y. Kasai, K. Hashimoto, J. Phys. Chem. A 109 (2005) 1836–1842.
[46] A. Brown, R.H. Tipping, in: C. Camy-Peyret, A.A. Vigasin (Eds.), Weakly Interacting Molecular Pairs: Unconventional Absorbers of Radiation in the Atmosphere, Kluwer Academic Publishers, London, 2003, pp. 93–97.
[47] H.J. Liebe, Int. J. Infrared Milli. Waves 5 (1984) 207–227.
[48] T. Kuhn, A. Bauer, M. Godon, S. Bühler, K. Kunzi, J. Quant. Spectrosc. Radiat. Transfer 74 (2002) 545–562.
[49] M.A. Koshelev, E.A. Serov, V.V. Parshin, M.Yu. Tretyakov, J. Quant. Spectrosc. Radiat. Transfer 112 (2011) 2704–2712.
[50] H.J. Liebe, G.A. Hufford, M.G. Cotton, AGARD Conf. Proc. 542 (1993) 3.1–3.10.
[51] J. Lamouroux, R.R. Gamache, A.L. Laraia, Q. Ma, R.H. Tipping, J. Quant. Spectrosc. Radiat. Transfer 113 (2012) 951–960.
[52] D.M. Dennison, Rev. Mod. Phys. 12 (1940) 175–214.
[53] H.J. Liebe, Int J. Infrared Milli. Waves 10 (1989) 631–650.
[54] H.J. Liebe, P.W. Rosenkranz, G.A. Hufford, J. Quant. Spectrosc. Radiat. Transfer. 48 (1992) 629–643.
[55] D.S. Makarov, M.Yu. Tretyakov, P.W. Rosenkranz, J. Quant. Spectrosc. Radiat. Transfer 112 (2011) 1420–1428.
[56] M.A. Koshelev, I.N. Vilkov, M.Yu. Tretyakov, J. Quant. Spectrosc. Radiat. Transfer 154 (2015) 24–27.
[57] S.G. Kukolich, J. Chem. Phys. 50 (1969) 3751–3755.
[58] C.H. Townes, F.R. Merritt, Phys. Rev. 70 (1946) 558–559.
[59] H.J. Liebe, M.C. Thompson, T.A. Dillon, J. Quant. Spectrosc. Radiat. Transfer 9 (1969) 31–47.
[60] H.J. Liebe, T.A. Dillon, J. Chem. Phys. 50 (1969) 727–732.
[61] T. Kasuga, H. Kuze, T. Shimizu, J. Chem. Phys. 69 (1978) 5195–5198.
[62] G. Cazzoli, C. Puzzarini, G. Buffa, O. Tarrini, J. Quant. Spectrosc. Radiat. Transfer 105 (2007) 438–449.
[63] G.W. King, R.M. Hainer, Phys. Rev. 71 (1947) 433–443.
[64] W.C. King, W. Gordy, Phys. Rev. 93 (1954) 407–412.
[65] J.R. Rusk, J. Chem. Phys. 43 (1965) 2919–2920.
[66] L. Frenkel, D. Woods, Proc IEEE. 54 (1966) 498–505.
[67] C.O. Hemmi, A.W. Straiton, Radio Sci. 4 (1969) 9–15.
[68] R. Emery, Infrared Phys. 12 (1972) 65–79.
[69] S.A. Zhevakin, A.P. Naumov, IzvVUZov Radiofizika 6 (1963) 674–694 (in Russian).
[70] E.P. Gross, Phys. Rev. 97 (1955) 395–403.
[71] A. Bauer, M. Godon, B. Duterage, J. Quant. Spectrosc. Radiat. Transfer 33 (1985) 167–175.
[72] A. Bauer, M. Godon, M. Kheddar, J.-M. Hartmann, J. Quant. Spectrosc. Radiat. Transfer 41 (1989) 49–54.
[73] G.Yu. Golubiatnikov, J. Mol. Spectrosc. 230 (2005) 196–198.
[74] T.M. Goyette, F.C. De Lucia, J. Mol. Spectrosc. 143 (1990) 346–358.
[75] A.F. Krupnov, V.N. Markov, Atmos. Oceanic Opt. 5 (1992) 140–141.
[76] A.F. Krupnov, in: G.W. Chantry (Ed.), Modern Aspects of Microwave Spectroscopy, Academic Press, London, 1979, pp. 217–256.
[77] M.Yu. Tretyakov, A.F. Krupnov, M.A. Koshelev, D.S. Makarov, E.A. Serov, V.V. Parshin, Rev. Sci. Instr. 80 (2009) 093106.
[78] A.F. Krupnov, M.Yu. Tretyakov, V.V. Parshin, V.N. Shanin, S.E. Myasnikova, J. Mol. Spectrosc. 202 (2000) 107–115.
[79] Yu.A. Dryagin, A.G. Kislyakov, L.M. Kukin, A.I. Naumov, L.I. Fedoseev, Radiophys. Quant. Electron. (Soviet Radiophysics) 9 (1966) 624–627.
[80] V.Ya. Ryadov, N.I. Furashov, Radiophys. Quantum Electron. 18 (1975) 256–266.
[81] S.L. Cruz-Pol, C.S. Ruf, S.J. Keihm, Radio Sci. 33 (1998) 1319–1333.
[82] V.H. Payne, J.S. Delamere, K.E. Cady-Pereira, R.R. Gamache, J.-L. Moncet, E.J. Mlawer, S.A. Clough, I.E.E.E. Trans, Geosci. Rem. Sens. 46 (2008) 3601–3617.
[83] H.C. Pumphrey, S. Bühler, J. Quant. Spectrosc. Radiat. Transfer 64 (2000) 421–437.
[84] F.T. Barath, M.C. Chavez, R.E. Cofield, D.A. Flower, M.A. Frerking, M.B. Gram, W.M. Harris, J.R. Holden, R.F. Jarnot, W.G. Kloezeman, G.J. Klose, G.K. Lau, M.S. Loo, B.J. Maddison, R.J. Mattauch, R.P. McKinney, G.E. Peckham, H.M. Pickett, G. Siebes, F.S. Soltis, R.A. Suttie, J.A. Tarsala, J.W. Waters, W.J. Wilson, J. Geophys. Res. 98 (1993) 10751–10762.
[85] C.L. Croskey, N. Kampfer, R.M. Belivacqua, G.K. Hartmann, K.F. Kunzi, P.R. Schwartz, J.J. Olivero, S.E. Puliafito, C. Aellig, G. Umlauft, W.B. Waltman, W. Degenhardt, I.E.E.E. Trans, Microwave Theory Technol. 40 (1992) 1090–1100.
[86] R.R. Gamache, R. Lynch, S.P. Neshyba, J. Quant. Spectrosc. Radiat. Transfer 59 (1998) 319–335.
[87] R.R. Gamache, J.M. Hartmann, Can. J. Chem. 82 (2004) 1013–1027.
[88] R.R. Gamache, J.M. Hartmann, J. Quant. Spectrosc. Radiat. Transfer 83 (2004) 119–147.
[89] R.R. Gamache, J. Fischer, J. Quant. Spectrosc. Radiat. Transfer 78 (2003) 289–304.
[90] R.R. Gamache, J. Fischer, J. Quant. Spectrosc. Radiat. Transfer 78 (2003) 305–318.
[91] R.A. Toth, L.R. Brown, C. Plymate, J. Quant. Spectrosc. Radiat. Transfer 59 (1998) 529–562.
[92] R.A. Toth, L.R. Brown, J. Mol. Spectrosc. 218 (2003) 135–150.
[93] R.A. Toth, J. Quant. Spectrosc. Radiat. Transfer (2005) 1–50.
[94] R.A. Toth, L.R. Brown, M.A.H. Smith, V.M. Devic, D.C. Benner, M. Dulick, J. Quant. Spectrosc. Radiat. Transfer 101 (2006) 339–366.
[95] M. Birk, G. Wagner, J. Quant. Spectrosc. Radiat. Transfer 113 (2012) 889–928.
[96] V.Yu. Katkov, B.A. Sverdlov, N.I. Furashov, Radiophys. Quantum Electron. 38 (1995) 835–844.
[97] T. Manabe, R.O. Debolt, H.J. Liebe, I.E.E.E. Trans, Anten. Propag. 37 (1989) 262–266.
[98] E.R. Westwater, J.B. Snider, M.J. Falls, I.E.E.E. Trans, Anten. Propag. 38 (1990) 1569–1580.
[99] D.D. Turner, M.P. Cadeddu, U. Löhnert, S. Crewell, A.M. Vogelmann, I.E.E.E. Trans, Geosci. Rem. Sens. 47 (2009) 3326–3337.
[100] V.H. Payne, E.J. Mlawer, K.E. Cady-Pereira, J.-L. Moncet, I.E.E.E. Trans, Geosci. Rem. Sens. 49 (2011) 2194–2208.
[101] H.J. Liebe, D.H. Layton, NTIA Rep. No. 87-224, Natl. Telecommun. And Inf. Admin., Boulder. Colo., 1987.
[102] A. Bauer, B. Duterage, M. Godon, J. Quant. Spectrosc. Radiat. Transfer 36 (1986) 307–318.
[103] A. Bauer, M. Godon, J. Quant. Spectrosc. Radiat. Transfer 46 (1991) 211–220.
[104] M. Godon, J. Carlier, A. Bauer, J. Quant. Spectrosc. Radiat. Transfer 47 (1992) 275–285.
[105] A. Bauer, M. Godon, J. Carlier, Q. Ma, R.H. Tipping, J. Quant. Spectrosc. Radiat. Transfer 50 (1993) 463–475.
[106] A. Bauer, M. Godon, J. Carlier, Q. Ma, J. Quant. Spectrosc. Radiat. Transfer 53 (1995) 411–423.
[107] A. Bauer, M. Godon, J. Carlier, R.R. Gamache, J. Mol. Spectrosc. 176 (1996) 45–57.
[108] A. Bauer, M. Godon, J. Carlier, R.R. Gamache, J. Quant. Spectrosc. Radiat. Transfer 59 (1998) 273–285.
[109] M. Godon, A. Bauer, R.R. Gamache, J. Mol. Spectrosc. 202 (2000) 293–302.
[110] A. Bauer, M. Godon, J. Quant. Spectrosc. Radiat. Transfer 69 (2001) 277–290.

[111] N.I. Furashov, V.Y. Katkov, V. Ryadov, Int. J. Infrared Milli. Waves 5 (1984) 971–984.
[112] N.I. Furashov, V.Y. Katkov, Int. J. Infrared Milli. Waves 6 (1985) 751–764.
[113] D.S. Makarov, M.Yu. Tretyakov, C. Boulet, J. Quant. Spectrosc. Radiat. Transfer 124 (2013) 1–10.
[114] M.Yu. Tretyakov, M.A. Koshelev, I.N. Vilkov, V.V. Parshin, E.A. Serov, J. Quant. Spectrosc. Radiat. Transfer 114 (2013) 109–121.
[115] A.I. Meshkov, F.C. De Lucia, J. Quant. Spectrosc. Radiat. Transfer 108 (2007) 256–276.
[116] G. Cazzoli, C. Puzzarini, G. Buffa, O. Tarrini, in: A. Perrin, N.B. Sari-Zizi, J. Demaison (Eds.), Remote Sensing of the Atmosphere for Environmental Security, Springer, Netherlands, 2005, pp. 237–255.
[117] G.Yu. Golubiatnikov, V.N. Markov, A. Guarnieri, R. Knoechel, J. Mol. Spectrosc. 240 (2006) 251–254.
[118] J. Tennyson, P.F. Bernath, L.R. Brown, A. Campargue, A.G. Csaszar, L. Daumont, R.R. Gamache, J.T. Hodges, O.V. Naumenko, O.L. Polyansky, L.S. Rothman, R.A. Toth, A.C. Vandaele, N.F. Zobov, A.R. Al Derzi, C. Fabri, A.Z. Fazliev, T. Furtenbacher, I.E. Gordon, L. Lodi, I.I. Mizus, J. Quant. Spectrosc. Radiat. Transfer 117 (2013) 29–58.
[119] O.L. Polyansky, A.A. Kyuberis, L. Lodi, J. Tennyson, N.F. Zobov, Mon. Not. R. Astron. Soc. (2016) (in preparation).
[120] L. Lodi, J. Tennyson, O.L. Polyansky, J. Chem. Phys. 135 (2011) 034113.
[121] H.M. Pickett, J. Chern. Phys. 73 (1980) 6090–6094.
[122] H.J. Liebe, V.L. Wolfe, D.A. Howe, Rev. Sci. Instrum. 55 (1984) 1702–1705.
[123] S. Payan, J. De La Noe, A. Hauchecorne, C. Camy-Peyret, CR Phys. 6 (2005) 825–835.
[124] V.V. Parshin, M.Yu. Tretyakov, M.A. Koshelev, E.A. Serov, Radiophys. Quantum Electron. 52 (2009) 525–535.
[125] M.Yu. Tretyakov, V.V. Parshin, V.N. Shanin, S.E. Myasnikova, M.A. Koshelev, A. F. Krupnov, J. Mol. Spectrosc. 208 (2001) 110–112.
[126] M.Yu. Tretyakov, G.Yu. Golubiatnikov, V.V. Parshin, M.A. Koshelev, S.E. Myasnikova, A.F. Krupnov, P.W. Rosenkranz, J. Mol. Spectrosc. 223 (2004) 31–38.
[127] M.Yu. Tretyakov, M.A. Koshelev, V.V. Dorovskikh, D.S. Makarov, P.W. Rosenkranz, J. Mol. Spectrosc. 231 (2005) 1–14.
[128] M.Yu. Tretyakov, M.A. Koshelev, I.A. Koval, V.V. Parshin, L.M. Kukin, L.I. Fedoseev, Yu.A. Dryagin, A.F. Andriyanov, J. Mol. Spectrosc. 241 (2007) 109–111.
[129] M.A. Koshelev, M.Yu. Tretyakov, G.Yu. Golubiatnikov, V.V. Parshin, V.N. Markov, I.A. Koval, J. Mol. Spectrosc 241 (2007) 101–108.
[130] D.S. Makarov, I.A. Koval, M.A. Koshelev, V.V. Parshin, M.Yu. Tretyakov, J. Mol. Spectrosc. 252 (2008) 242–243.
[131] M.Yu. Tretyakov, M.A. Koshelev, D.S. Makarov, M.V. Tonkov, Instrum. Exp. Tech. 51 (2008) 78–88.
[132] G.Yu. Golubiatnikov, S.P. Belov, I.I. Leonov, A.F. Andrianov, I.I. Zinchenko, A.V. Lapinov, V.N. Markov, A.P. Shkaev, A. Guarnieri, Radiophys. Quantum Electron. 56 (2014) 599–609.
[133] P.W. Rosenkranz, Radio Sci. 34 (1999) 1025.
[134] C.L. Verdes, S.A. Bühler, A. Perrin, J.-M. Flaud, J. Demaison, G. Wlodarczak, J.-M. Colmont, G. Cazzoli, C. Puzzarini, J. Mol. Spectrosc. 229 (2005) 266–275.